THESIS FOR THE DEGREE OF LICENTIATE OF ENGINEERING

Unconventional Modulation of Diarylethene Photoswitches

WERA LARSSON

Department of Chemistry and Chemical Engineering
CHALMERS UNIVERSITY OF TECHNOLOGY
Gothenburg, Sweden 2022

Unconventional Modulation of Diarylethene Photoswitches
WERA LARSSON

Supervisor: Bo Albinsson
Examiner: Jerker Mårtensson

Licentiatuppsatser vid Institutionen för kemi och kemiteknik
Chalmers tekniska högskola
Nr 2022:10

Department of Chemistry and Chemical Engineering
Chalmers University of Technology
SE-412 96 Gothenburg
Sweden
Telephone +46 31 772 1000

Printed by Department of Chemistry and Chemical Engineering
Gothenburg, Sweden 2022

Unconventional Modulation of Diarylethene Photoswitches

Wera Larsson
Department of Chemistry and Chemical Engineering
Chalmers University of Technology

Abstract

Light can be manipulated and modulated to fit a particular need or application, such as overcoming a spectral mismatch when facilitating a high energy photochemical reaction. This can be of use in various applications, including solar energy conversion and biological contexts. Photochromic molecules, or molecular photoswitches, undergo photoisomerization reactions when subjected to light of different wavelengths, which can be tracked *in situ* by spectroscopic techniques such as UV-vis absorption and fluorescence. In this thesis, the photoisomerization and fluorescence of diarylethene photoswitches are modulated by three unconventional methods. The methods are unconventional in the sense that the photochemical processes are not induced by direct excitation. Instead, the photochemistry in the three included papers is respectively facilitated by rapid modulation of light that is not absorbed by the fluorescent isomer, triplet sensitization using hybrids of nanocrystals and organic mediators, or triplet-triplet annihilation photon upconversion. While further improvements are needed for these methods to reach their full potential, the findings in this thesis brings us closer to visible-light control of high energy photochemical transformations.

Keywords: photochemistry, photochromic molecules, molecular photoswitches, diarylethene, triplet sensitization, nanocrystals, photon upconversion, triplet-triplet annihilation

List of Publications

This thesis is based on the following papers:

Paper I

Rapid amplitude-modulation of a diarylethene photoswitch: en route to contrast-enhanced fluorescence imaging. Gaowa Naren,[‡] Wera Larsson,[‡] Carlos Benitez-Martin, Shiming Li, Ezequiel Pérez-Inestrosa, Bo Albinsson and Joakim Andréasson. *Chemical Science, 2021, 12, 7073-7078*

Paper II

A General Approach for All-visible-light Switching of Diarylethenes through Triplet Sensitization using Semiconducting Nanocrystals. Lili Hou, Wera Larsson, Stefan Hecht, Joakim Andréasson and Bo Albinsson. *Submitted manuscript*

Paper III

Diarylethene isomerization using triplet-triplet annihilation photon upconversion. Wera Larsson, Masakazu Morimoto, Masahiro Irie, Joakim Andréasson and Bo Albinsson. *Submitted manuscript*

My contribution to the papers

Paper I: Performed most of the photophysical measurements and most of the data analysis together with G.N., and some alone. Wrote part of the manuscript. [‡]Shared first authorship together with G.N. All synthesis related work was done by S.L. and microscopy measurements were done by C.B.M.

Paper II: Performed some of the photophysical measurements together with L.H. and did part of the data analysis. Contributed to the manuscript. All synthesis related work was done by L.H. and S.H.

Paper III: Performed all of the photophysical measurements and all data analysis. Planned the experiments together with J.A. and B.A. Wrote most of the manuscript. All synthesis related work was done by M.M. and M.I.

List of Abbreviations

3-PCA	Phenanthrene-3-carboxylic acid
CCD	Charge-coupled device
CdS	Cadmium sulfide
DAE	Diarylethene
DET	Dexter energy transfer
DPA	9,10-diphenylanthracene
FRET	Förster resonance energy transfer
HOMO	Highest occupied molecular orbital
IC	Internal conversion
IR	Infrared
ISC	Intersystem crossing
LUMO	Lowest unoccupied molecular orbital
NC	Nanocrystal
ns-TA	Nanosecond transient absorption
OLID	Optical lock-in detection
PMT	Photomultiplier tube
PSS	Photostationary state
PtOEP	Platinum octaethylporphyrin
TA	Transient absorption
TCSPC	Time correlated single photon counting
TET	Triplet energy transfer
TTA	Triplet-triplet annihilation
TTA-PUC	Triplet-triplet annihilation photon upconversion
UC	Upconversion
UV	Ultraviolet
VR	Vibrational relaxation

Contents

1

Introduction

Manipulation and modulation of light to match human needs have great importance in fields like solar energy conversion and biological applications. Sunlight is highly abundant on Earth,[1] but there is a spectral mismatch between the available sunlight and the light that is needed in solar energy applications. One such example is the light needed in photovoltaics. The most common solar cells as of today are single junction silicon solar cells, with a bandgap of 1.1 eV (i.e. approximately 1100 nm).[2] This means that photons with this specific energy are ideal to use in these types of solar cells, but there are large portions of the sunlight reaching Earth that does not match this bandgap. The light with lower energy cannot be utilized at all, while the light having higher energy results in thermal losses. All together, this spectral mismatch limits the theoretical efficiency of single junction solar cells to 32%.[3] Another spectral mismatch relating to solar energy applications is the energy of light needed to produce solar fuels. One such example is photoinduced catalytic water splitting, which require photons with high energy in order to be efficient.[4,5] This means that mainly ultraviolet (UV) light is feasible in this type of applications, but a large portion of the UV light coming from the sun is absorbed by the ozone layer and does not reach Earth.

In the biological applications relevant for this thesis, more factors concerning UV light come into play. First of, photodegradation (also relevant in solar energy applications) as a result of photooxidation is triggered by UV radiation. Another problem with UV light is that it does not penetrate tissue very well, since the shorter the wavelength the shallower the penetration depth.[6,7] A third UV light related factor calling for light manipulation is that it induces autofluorescence when imaging cells in fluorescence microscopy, which lowers the signal-to-background ratio.

A solution to the spectral mismatch related issues mentioned above is to alter and match the available light in different ways to control photochemical processes. The photochemical processes that are the focus of this thesis are reversible photoisomerization of diarylethene (DAE)[8–10] photochromic molecules, and controlling their fluorescence. Here, this family of molecules serves both as a suggested tool for further applications, and as model compounds to display unconventional control of photochemical reactions. This thesis spans over three unconventional ways of modulating DAEs, unconventional meaning that controlling the isomerization and fluorescence of the DAEs is not done by merely irradiating with light that is directly absorbed by the isomer that we want to photoisomerize and/or have fluorescing. In the three papers included in this thesis, this is instead facilitated respectively by rapid modulation of light that is not absorbed by the fluorescent isomer, triplet sensitization using hybrids of nanocrystals (NCs) and organic mediators, or triplet-triplet annihilation photon upconversion (TTA-PUC).[11]

1.1 Aim

The focus of this thesis is three unconventional ways of modulating DAEs, as a way to use and manipulate light to match our needs. Paper I focuses on rapid fluorescence modulation of a DAE derivative in water, and by using lock-in amplification this fluorescence can be singled out from a bright background. This process has shown great potential to improve fluorescence microscopy. In Paper II, hybrids of NCs and organic mediators are used to reversibly isomerize DAEs using only visible light through triplet sensitization. Photoisomerization of DAEs typically requires UV light, hence this suggested process removes problems arising from using UV light such as photodegradation and lack of tissue penetration. The focus of Paper III is also to use visible light to reversibly isomerize DAEs, but instead uses the process of TTA-PUC to facilitate this. In this paper, both reversible photoisomerization and fluorescence can be triggered using a single visible light source. As an addition to this single light source control of the DAEs, this paper aims to act as a step foward on the path toward controlling photochemical reactions using the abundant visible sunlight by the means of TTA-PUC.

2

Theory

Interactions between light and matter are central to all the projects included in this work, and the fundamental theory behind this will be presented in this chapter. Other concepts that are relevant for this thesis are also introduced, like energy transfer, diarylethene photoswitches, triplet sensitization and TTA-PUC.

2.1 Light and matter

Light can be described both as an oscillating electric and magnetic (electromagnetic) field, and as a particle. These two ways of describing light constitutes the wave-particle duality. This duality is evident in the definition of the energy of a light particle, photon:

$$E = \frac{hc}{\lambda} = h\nu \tag{2.1}$$

where h is the Planck constant, c is the speed of light, λ is the wavelength and ν is the frequency of the electromagnetic field.[12] Equation (2.1) shows that the energy that is carried by a photon is discrete.

When talking about light, it is often divided into different wavelength regions, three of them being relevant for the methods used in this thesis. Visible light has a wavelength range of 400-750 nm, and the wavelength regions surrounding this spectral region are referred to as UV light (shorter wavelengths) and infrared (IR) light (longer wavelengths). Interaction between light and matter can result in absorption and scattering. When visible light is absorbed by for example a molecule, an electron in the molecule is promoted to an orbital with higher energy, leaving the molecule in a higher electronic excited state. For this to occur, Bohr's frequency condition has to apply. This means that the energy of

the absorbed photon must match the energy difference between the two states.[12]

An important property of electrons is their spin, with values being either $\pm\frac{1}{2}$ (commonly referred to as spin up or down). The Pauli exclusion principle states that two electrons occupying the same molecular orbital must have opposite spin, meaning that the electrons are paired. If all electrons in a molecule are paired, the molecule is said to be in a singlet state and the total spin (S) is zero. When two electrons in different molecular orbitals are unpaired, they instead have parallel spin and the molecule is said to be in a triplet state with a total spin of one. The words singlet and triplet stems from the multiplicity ($2S+1$) of the electronic states, which is one for singlet states and three for triplet states. Most molecules have a singlet ground state, which will also be the case in the example presented in the following paragraph.

Figure 2.1 shows a Jablonski diagram displaying some of the photophysical processes that can occur when a photon is absorbed by a molecule. Upon absorption (blue arrow), the molecule is typically excited from its singlet ground state (S_0) to a higher vibrational level of its singlet excited state (S_1) and absorption occurs in less than a femtosecond. The molecule then relaxes to S_1 by vibrational relaxation (VR) (wavy black arrow), and from this energy level the molecule can decay to S_0 through several radiative and non-radiative pathways. A non-radiative decay pathway is through internal conversion (IC) (dashed black arrow) to a high vibrational energy level of S_0, followed by VR to the lowest vibrational energy level. The energy can also be released as light through fluorescence (green arrow), which occurs on a timescale of nanoseconds. Another radiative decay pathway is phosphorescence (red arrow) from the first triplet excited state (T_1) to S_0. For this to occur, the energy first has to be transferred through intersystem crossing (ISC) from S_1 to T_1. Both ISC and phosphorescence require a spin flip, and are hence said to be spin-forbidden processes. This results in the lifetime of phosphorescence (i.e. the time the molecule will reside in its excited state) being longer than that of fluorescence with typical timescales of micro- to milliseconds. The molecule can also decay non-radiatively from T_1 through ISC followed by VR.

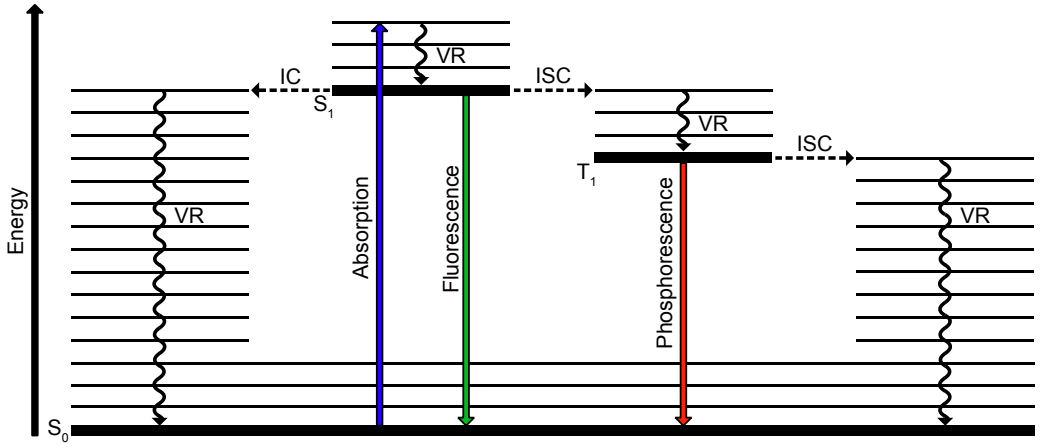

Figure 2.1: Jablonski diagram showing a singlet ground state (S_0) together with the first singlet (S_1) and triplet excited states (T_1) all depicted as thick black horizontal lines, together with different photophysical processes. The photophysical processes (arrows) shown in the figure are absorption, vibrational relaxation (VR), fluorescence, internal conversion (IC), intersystem crossing (ISC), and phosphorescence. Thin black horizontal lines represent vibrational energy levels.

There is often a need to quantify photophysical processes, and two common ways of doing this is to measure the rate of a certain process through time-resolved measurements and to measure the quantum yield (Φ). The latter describe how efficient the process at hand is compared to all other possible processes. This is described for a photophysical process in Equation (2.2).

$$\Phi_i = \frac{number\ of\ events}{number\ of\ photons\ absorbed} \tag{2.2}$$

A quantum yield that is relevant in this thesis is the fluorescence quantum yield, in which the fluorescence is compared to all other possible decay pathways after an absorption event. Another central quantum yield is the isomerization quantum yield, which relates the amount of isomerization events to the number of absorbed photons. The latter will be described in more detail in Section 2.3.

2.2 Energy transfer

The previous section described decay pathways for excited state molecules, but the energy can also be transferred to other molecules. There are two main types

of non-radiative energy transfer mechanisms, namely Förster resonance energy transfer (FRET)[13] and Dexter energy transfer (DET).[14] The former is based on dipole-dipole interactions between a donor and an acceptor molecule, and does not involve any electron exchange. This on the other hand applies to DET, in which the energy of an electronically excited donor is transferred to a ground state acceptor through electron exchange. Figure 2.2 illustrates a triplet energy transfer (TET) event from a triplet excited donor molecule (^{3}D*) to a ground state acceptor (A) through DET, resulting in a ground state donor molecule (D) and a triplet excited acceptor molecule (^{3}A*). The electron exchange involves both the highest occupied molecular orbital (HOMO) and the lowest unoccupied molecular orbital (LUMO) of the two molecules. Although the spin multiplicity of both the donor and acceptor molecules change during this TET, the total spin angular momentum of the whole system is preserved which makes it a spin-allowed process.

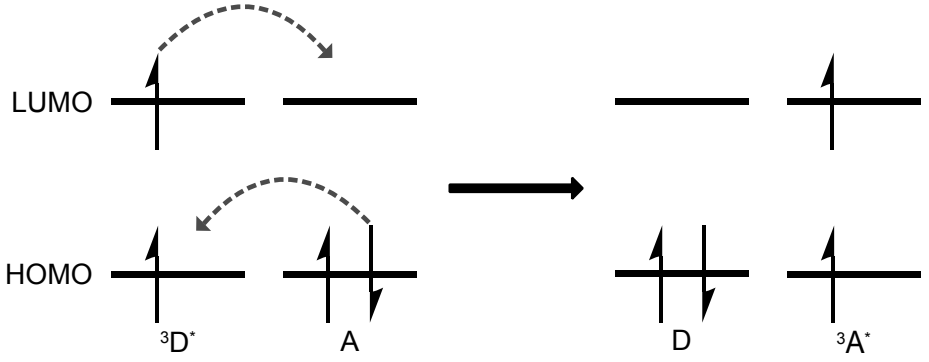

Figure 2.2: Schematic illustration of triplet energy transfer through the Dexter energy transfer mechanism. An electron exchange occurs involving an electron from the LUMO of the triplet excited donor molecule (^{3}D*) and an electron from the HOMO of the ground state acceptor (A), resulting in a ground state donor molecule (D) and a triplet excited acceptor molecule (^{3}A*).

2.3 Diarylethene molecular photoswitches

Photochromic molecules, also referred to as molecular photoswitches, are molecules that can undergo a reversible transformation between two forms referred to as isomers. This reversible transformation, or isomerization, is generally photoinduced in both directions, but can for some photoswitches also occur thermally in

one of the directions. Isomerization results in structural changes that give rise to different absorption and fluorescence spectra for the two isomers together with other differences in properties including refractive indices, dielectric constants and redox potentials.[8,10,15] One of the major families of photochromic molecules is the previously briefly mentioned DAEs, and all molecular photoswitches used in this thesis belong to this group of compounds. As of today, many different DAEs have been synthesized and they are used in various applications such as optical memories,[16] organic light-emitting transistors,[17] and bioimaging.[18] One of the reasons behind their popularity is that they possess properties like thermal stability, high fatigue-resistance, sensitivity, and rapid response together with reactivity in the solid state.[15,19]

The two isomers are commonly referred to as the open and the closed form, and an isomerization scheme for the DAE referred to as DAE2 in Paper III is shown in Figure 2.3. DAEo (left structure in the isomerization scheme) refers to the colorless open isomer, and it absorbs mainly in the UV region. The colored closed isomer DAEc (right structure in the isomerization scheme) absorbs strongly also in the visible region, hence UV light can be used to facilitate the ring-closing reaction while visible light can be used to facilitate the reverse ring-opening reaction.

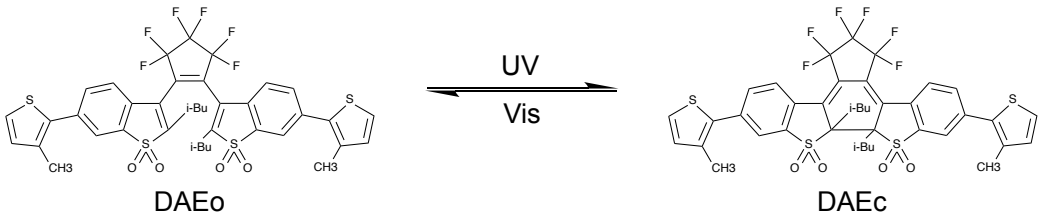

Figure 2.3: Structures and isomerization scheme of the DAE referred to as DAE2 in Paper III. UV light is used to isomerize from the open isomer DAEo to the closed isomer DAEc, and visible light is used to facilitate the reverse isomerization.

Isomerization is governed by cyclization reactions, during which a rearrangement of single and double bonds occur. This structural change influences the emission properties of the DAEs, and all DAEs used in this thesis have one strongly fluorescent isomer. In Paper I, it is the open form that is fluorescent meaning that UV light triggers the fluorescence. The DAEs used in Paper II and

Paper III, exemplified in Figure 2.3, are fluorescent in their closed forms.

2.4 Triplet sensitization

Sensitization is the process in which a molecule (sensitizer) absorbs light and transfers its excited state energy to a nearby molecule, leaving the sensitizer in its ground state.[20,21] A triplet sensitizer is excited to its singlet excited state which then relaxes to a triplet excited state, and an efficient sensitizer needs to have a high molar absorptivity and fast ISC. To further ensure an efficient sensitization process, the singlet and triplet excited state energies of the sensitizer ought to be close to each other to avoid thermal losses. The energy transfer then occurs through TET, resulting in a triplet excited acceptor. Both the sensitizer and the acceptor molecule have to be in close proximity to each other for sensitization to occur, which can be achieved either through attaching the sensitizer to the acceptor[22–25] or having them mixed in solution. In the latter case, the sensitization is diffusion-controlled which means that the triplet lifetime of the sensitizer has to be sufficiently long (typically in the microsecond to millisecond regime) to allow for the sensitization to occur. Another thing to note here is that triplet states are efficiently quenched by molecular oxygen, implying that sensitization often has to be done in an oxygen free environment.[26–28]

A route to achieve all-visible-light switching of DAEs is to drive the cyclization reaction along the triplet manifold through sensitization, rather than singlet excitation of the open isomers. Since the first triplet excited state of the DAEs is lower in energy than the first singlet excited state, this process require less energy and can hence be triggered using light of longer wavelengths than direct UV light facilitated ring-closing. The use of visible light improves the fatigue resistance of repeated DAE izomerization, since photodegradation is shown to only occur on the singlet manifold.[29,30] This improved fatigue resistance is also shown in Paper II, where we used triplet sensitization from NCs/organic mediator hybrids to drive the ring-closing reaction of a group of DAEs.

2.5 Photon upconversion

Upconversion of light is a process where lower energy light is converted into light with higher energy. The photon upconversion process used in this thesis is triplet-triplet annihilation photon upconversion (TTA-PUC), in which two lower energy photons are converted into one higher energy photon through a series of energy transfer steps.[11] A Jablonski diagram showing the mechanism behind TTA-PUC is shown in Figure 2.4. TTA-PUC is initiated by absortion of light (green arrows) by a sensitizer molecule (S), leaving the sensitizer in its first singlet excited state (^{1}S*). This is followed by ISC to the first triplet excited state (^{3}S*), implying that a good sensitizer need to have a high rate of ISC to generate triplet excited states efficiently. The triplet energy of the sensitizer is then transferred to a ground state annihilator molecule (A) through TET leaving the annihilator in its first triplet excited state (^{3}A*). In the subsequent step, two triplet excited annihilators interact through triplet-triplet annihilation (TTA) leaving one annihilator in its ground state and one in its first singlet excited state (^{1}A*). Since both the TET and TTA processes are diffusion-controlled in liquid solutions, both the sensitizer and the annihilator need to have a sufficiently long triplet lifetime (typically in the microsecond to millisecond regime) for these processes to occur. The energy of the ^{3}A* state need to be at least half of that of the ^{1}A* state for this process to be energetically allowed. Finally, a photon of higher energy than the two absorbed by the sensitizers can be emitted as fluorescence (blue arrow) and the annihilator relaxes down to its ground state.

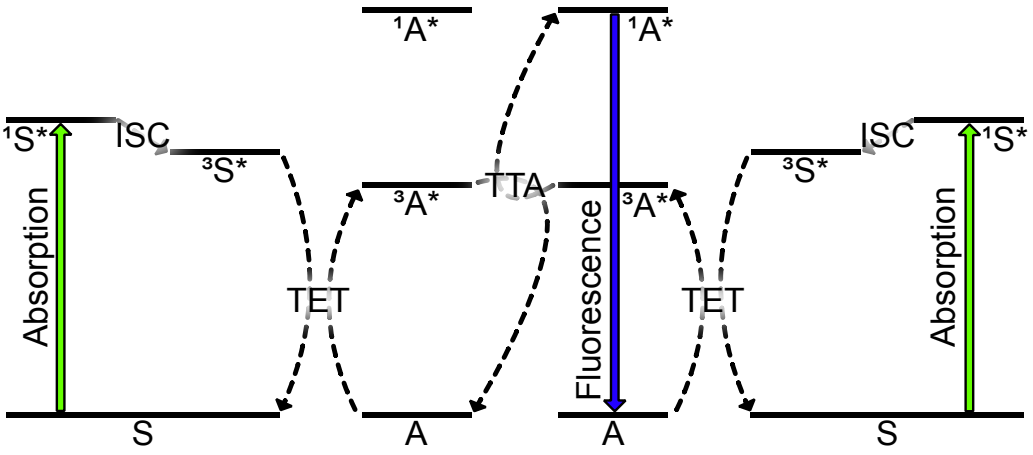

Figure 2.4: Jablonski diagram of the TTA-PUC process.

Since TTA-PUC combines two low energy photons to emit one higher energy photon, the quantum yield can by definition reach a theoretical maximum of 50%.[31] The highest reported upconversion quantum yield as of today is 42% for red-to-blue TTA-PUC,[32] while the highest reported visible-to-UV upconversion quantum yield is 17%.[33] Just as for the previously described triplet sensitization process, TTA-PUC relies on triplet excited states meaning that molecular oxygen acts as a quencher also for this process. Two of the suggested applications for TTA-PUC are to enhance the efficiency of solar cells[34–37] and to produce solar fuels,[38] which stems from the fact that TTA-PUC is an upconversion process that performs well under low-intensity noncoherent light such as sunlight.[39–41] This thesis does not focus on the mechanistic insights of TTA-PUC or on developing new sensitizers or annihilators, but rather to in Paper III use TTA-PUC as a tool to control photoisomerization of DAEs.

3

Spectroscopic methods

Optical spectroscopic techniques are the basis of the experimental work that has been conducted in this thesis. In this chapter, a brief presentation of the different techniques is presented together with examples of how they have been used.

3.1 UV-vis steady-state absorption spectroscopy

UV-vis steady-state absorption spectroscopy is a method in which the intensity of light transmitted through a sample is used to determine absorption at certain wavelengths. A typical setup is shown schematically in Figure 3.1. The probe light passes through a monochromator, after which the light intensity before, I_0, and after, I, the sample is measured by a reference detector and a sample detector respectively. These intensities are related to the absorbance, A, by the Lambert-Beer law[42] seen in Equation (3.1).

$$A = -log_{10}\left(\frac{I}{I_0}\right) = \varepsilon cl \tag{3.1}$$

As seen in this equation, the absorbance is also related to the molar absorptivity, ε, at the specific wavelength, the concentration, c, of the sample and the optical path length, l.

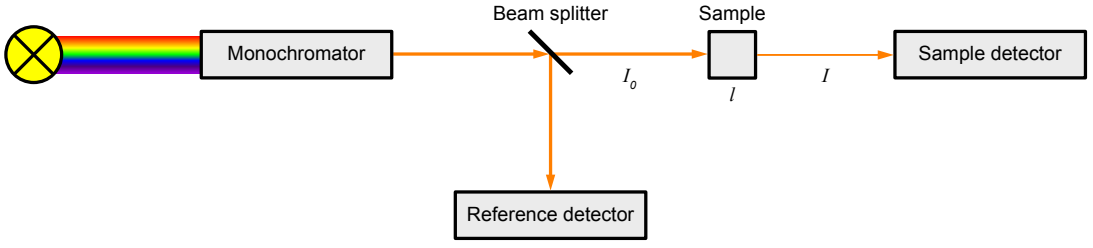

Figure 3.1: Schematic illustration of a setup used to measure steady-state absorption.

By allowing the monochromator to sweep over a range of wavelengths, an absorption spectrum can be obtained where the relative amplitude of the absorbance at different wavelengths is determined by the molar absorptivity. An absorption spectrum provides information about the presence of different species in a sample and their respective concentrations. It can also be used as a tool to determine reaction kinetics, by measuring the absorbance of a reacting species over time.

3.2 Steady-state emission spectroscopy

Determination of steady-state emission from a sample can be done in a setup similar to that used in UV-vis steady-state absorption spectroscopy. A schematic illustration of such a setup is shown in Figure 3.2. The sample is subjected to monochromatic light, either by using a white light combined with a monochromator or using a laser light source. Another monochromator is situated after the sample that is used to determine the wavelength of light that will be detected. Sweeping the excitation monochromator and detecting the emission intensity of only a single wavelength provides an excitation spectrum, which mimics the absorption spectrum of the emitting species. By instead sweeping the emission monochromator and keeping the excitation light fixed at a certain wavelength that is absorbed by the sample, an emission spectrum can be obtained.

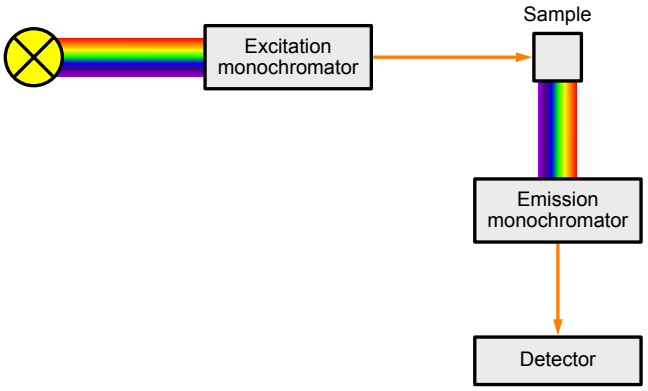

Figure 3.2: Schematic illustration of a setup used to measure steady-state emission.

Steady-state emission spectroscopy can be used to e.g. determine fluorescence quantum yields and study emission quenching. By measuring the emission intensity over time, one can also study reaction kinetics. Fluorescence spectroscopy

is a very sensitive measuring technique, and can hence be used to determine even smaller concentrations than absorption spectroscopy. As an example of the sensitivity, we show in Paper I how lock-in amplification can be used in combination with steady-state emission spectroscopy to detect a fluorescence modulated signal from a strongly fluorescent background.

3.3 Time-resolved spectroscopy

Fluorescence lifetime, τ, is a merit that describes how the emission intensity decays over time, and can be measured using time-resolved emission spectroscopy. The sample is excited by a short excitation pulse, and the emission decay is then recorded. Time correlated single photon counting (TCSPC) was used in this work to measure fluorescence lifetimes, and a schematic illustration of such a setup is shown in Figure 3.3. A pulsed laser diode is used as the excitation source, upon which the time needed for the first emitted photon to reach the detector is recorded. This is repeated for many pulses, and the recorded data is used to construct a histogram showing the decay of the emission intensity.

Nanosecond transient absorption (ns-TA) spectroscopy is another time-resolved measurement technique, which is used to study the absorption of excited states. A typical setup for this is shown in Figure 3.3. As for TCSPC, the sample is excited using a pulsed laser. The sample is also subjected to light from a continuous probe lamp, and the detector records the transmitted light with, A_+, and without, A_-, excitation from the pulsed laser. In the same way as in steady-state absorption spectroscopy, the difference in transmission is represented as absorbance which in the ns-TA spectroscopy case is represented as differential absorption seen in Equation (3.2).

$$\Delta A = A_+ - A_- \tag{3.2}$$

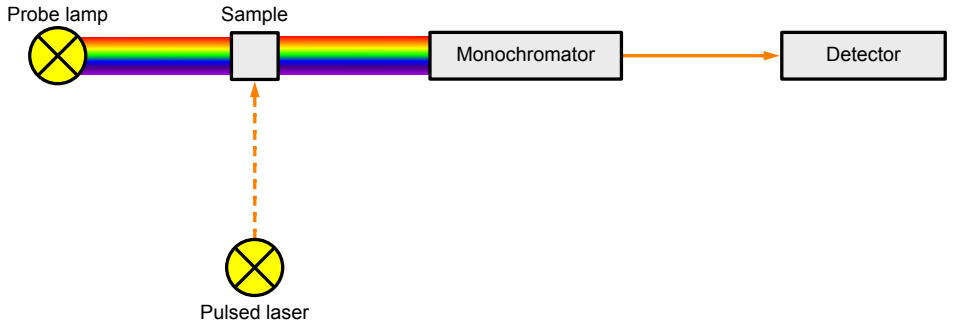

Figure 3.3: Schematic illustration of a setup used to measure time-resolved emission and transient absorption. Note that the probe lamp is not turned on when measuring emission, and that the type of detector used varies with the type of measurement that is performed.

Time-resolved decays at single wavelengths can be measured by selecting the wavelength of interest using a monochromator and recording the signal using a photomultiplier tube (PMT). An entire TA spectrum can be recorded by instead using a gated charged-coupled device (CCD) camera as a detector, and the time evolution of the spectral features can be investigated by varying the delay time.

4

Intensity modulation of a turn-off mode fluorescent DAE

DAEs that are only fluorescent in their open isomers but display no emission from their closed isomers, are called turn-off mode DAEs.[15] The fluorescence in the initial open-form decreases when the compound is subjected to UV irradiation, since UV light induces both fluorescence of DAEo and isomerization to DAEc. An asymmetric DAE referred to as Dasy is used in this project,[43] with Figure 4.1 showing the structures of the open (Dasy(o)) and closed isomers (Dasy(c)) in an isomerization scheme. Dasy is a water soluble molecule that displays a high fluorescence quantum yield of 0.21 in water for the open isomer. Although there is another DAE derivative that has a fluorescence quantum yield of the open isomer close to this value, the fluorescence of that derivative cannot be fully turned off upon UV light irradiation due to poor conversion to the closed isomer.[44] Dasy on the other hand can reach virtually 100% of Dasy(c) when subjected to UV light.

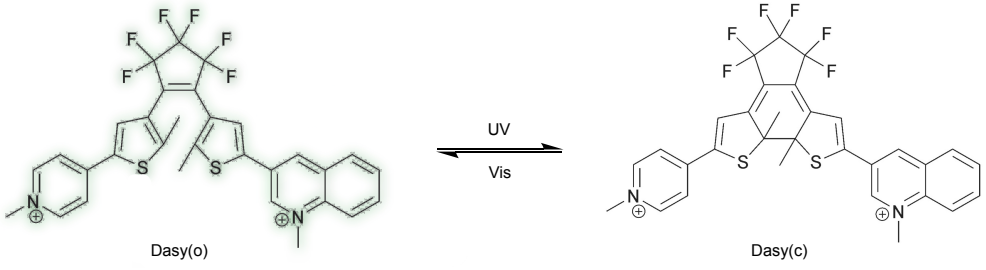

Figure 4.1: Structures and isomerization scheme of Dasy. UV light is used to isomerize from the open isomer Dasy(o) to the closed isomer Dasy(c), and visible light is used to facilitate the reverse isomerization. The green glow on Dasy(o) is there to visualize its UV light induced fluorescence.

Figure 4.2 shows the absorption spectra of Dasy(o) and Dasy(c) together with the Dasy(o) fluorescence in aqueous solution. Dasy(o) has its most redshifted absorption band centered at 351 nm, and mainly absorbs in the UV region, while Dasy(c) absorbs also in the visible region with an absorption band centered at 644 nm. The isomerization quantum yields are 0.44 for the ring-closing reaction and 0.0033 for the ring-opening reaction under 365 nm and 523 nm irradiation, respectively. As previously mentioned, the open isomer display strong fluorescence under UV light irradiation, and Dasy(o) has an emission maxima at 511 nm.

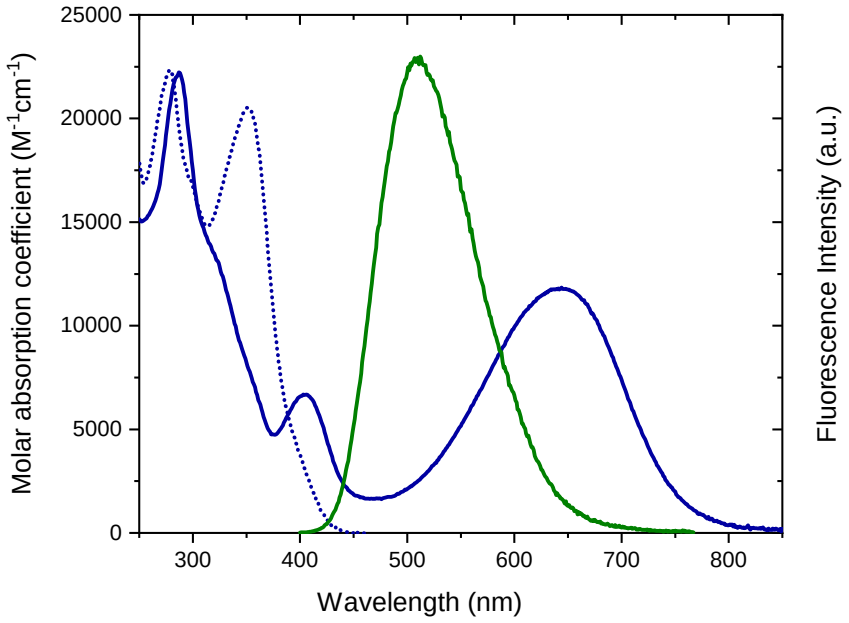

Figure 4.2: Absorption spectra of Dasy(o) (dotted blue line) and Dasy(c) (solid blue line) together with the emission spectrum of Dasy(o) (solid green line) in water.

The above mentioned properties, like water solubility, high fluorescence quantum yield in the colorless open form and the possibility to fully convert between the open and closed isomers make Dasy an excellent candidate for biological applications. In this project, the focus has been to enhance the contrast in fluorescence microscopy by rapid fluorescence modulation. A problem in fluorescence microscopy is to distinguish the desired fluorescence (typically from synthetic fluorescent probes) from undesired autofluorescence from the cells. This decreases the attainable contrast in fluorescence microscopy, since the signal-

to-background ratio is limited by the background emission. To distinguish the sought after fluorescence from the bright background, the excitation light can be modulated and optical lock-in detection (OLID)[45] can be used to record the amplitude modulated emission from the fluorescent probes. This only works if it is possible to modulate the probe emission, but not the autofluorescence. Previously reported examples suffer from only being demonstrated in organic solvents,[46,47] and requiring extensive synthetic sample preparation.[46–49] They have typically shown very low fluorescent quantum yields, low photostability and are fluorescent in their colorless open form which calls for extensive data processing to distinguish the probe signal from the background.[45,50,51] These factors are all accounted for when using Dasy, and as will be shown our modulation frequencies vastly exceed the previously reported ones that have been below 1 Hz.[45,48,49]

4.1 Rapid modulation

Amplitude modulation of Dasy fluorescence was done by continuously irradiating an aqueous solution of Dasy with UV light, eventually resulting in a photostationary state (PSS) consisting only of Dasy(c) and that the initial fluorescence is turned off. Exposing the sample to red light at this point without turning off the UV light triggers isomerization from Dasy(c) to Dasy(o), and at the new PSS resulting from the simultaneous irradiation of UV and red light the fluorescence is turned on again. By constant UV irradiation and modulation of the red light, the fluorescence of Dasy can be switched on and off as shown schematically in Figure 4.3. Although it is the UV light that induces the fluorescence, it is the modulation of light that is not absorbed by the fluorescent species that controls the fluorescence intensity. A_m in Figure 4.3 is the modulation amplitude, f_m is the modulation frequency and k_{obs} is the observed rate constant for reaching the PSS induced by simultaneous irradiation of Dasy(o) with UV and red light.

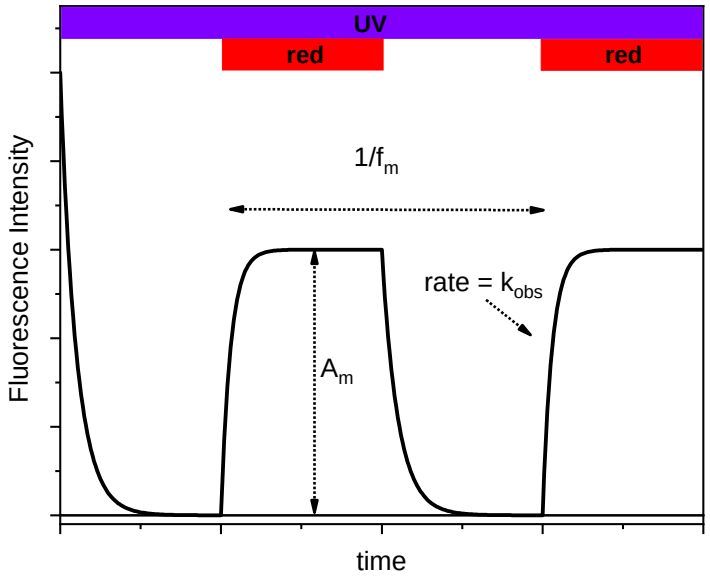

Figure 4.3: Schematic illustration of how Dasy is switched between the two photostationary states, when alternately irradiating the sample with only UV light and both UV light and red light simultaneously. f_m is the modulation frequency, A_m is the modulation amplitude and k_{obs} is the observed rate constant for the process of reaching the photostationary state resulting from simultaneous irradiation with UV and red light.

The amplitude modulation of Dasy(o) fluorescence is experimentally shown in Figure 4.4, for different modulation frequencies. In all three cases, a *ca.* 20 μM aqueous solution of Dasy was exposed to continuous 365 nm UV light ($\sim$30 mW) and square-wave modulated 660 nm red light ($\sim$40 mW). The red light was modulated with increasing frequencies: 10 Hz (left), 105 Hz (middle) and 205 Hz (right). At low frequencies, the modulation amplitude is constant upon variation since the irradiation times are long enough for the sample to fully isomerize between the two PSS. A further increase in f_m results in an initially dramatic decrease in A_m, which levels out at large modulation frequencies. This correlation between A_m and f_m is further described in Paper I.

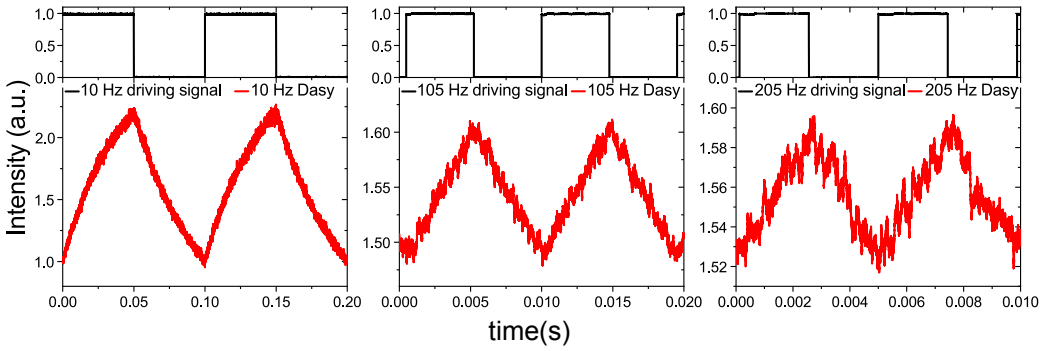

Figure 4.4: Amplitude modulation of Dasy in aqueous solution with modulation frequencies of 10 Hz (left), 105 Hz (middle) and 205 Hz (right). The samples were under constant 365 nm irradiation, and the 660 nm laser is modulated at different frequencies (black lines) inducing the fluorescence modulation of Dasy (red lines).

4.2 Background removal

OLID is a method that can be used to distinguish an alternating signal with a fixed frequency from a constant background, and as previously mentioned this could be used to enhance the contrast in fluorescence microscopy. After showing that the Dasy(o) fluorescence could be rapidly amplitude modulated, the next step was to try to distinguish the Dasy emission from a bright background. This was done by using a 450 nm light source, with its spectral profile shown in Figure 4.5 (blue line). A steady-state emission spectrum was recorded of Dasy(o) continuously excited by 365 nm light while simultaneously exposing the detector to the 450 nm light source (red line). It is clear that the 450 nm light source contribution to this spectrum is the dominating one. A comparative spectrum was recorded with Dasy(o) and the 450 nm light source, but this time the signal was recorded using OLID. Dasy was subjected to continuous irradiation of 365 nm light, together with 660 nm light modulated with a frequency of 10 Hz. The lock-in amplifier was adjusted to detect a 10 Hz signal, and the detector scanned the same wavelength region as was done when doing the steady-state measurement. This recording is shown as a green line in Figure 4.5, and it is evident that the continuous bright background light (the 450 nm light source) is completely filtered out and the resulting spectrum consists of only Dasy(o) emission (compare with Figure 4.2).

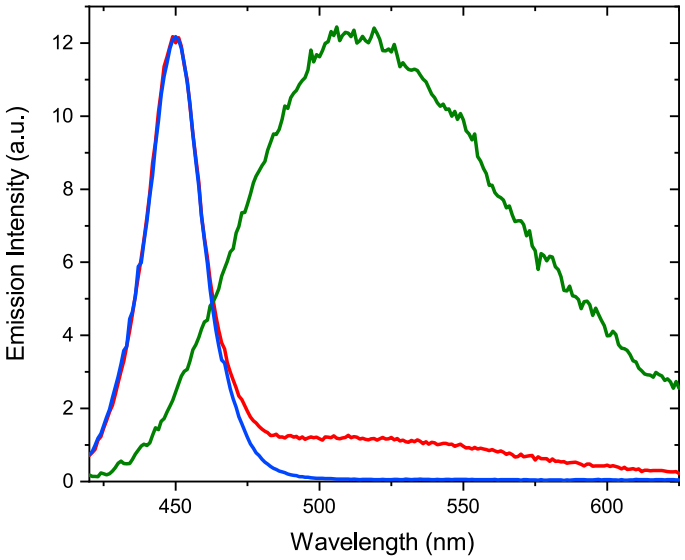

Figure 4.5: Spectral profile of the 450 nm light source (blue line), steady-state emission spectrum of Dasy fluorescence together with the 450 nm light source (red line), together with an amplitude-modulated spectrum of Dasy + 450 nm light source under 10 Hz modulation of the 660 nm laser and continuous 365 nm irradiation (green line). All spectra are normalized to a common maximum value.

We have shown that Dasy fluorescence can be rapidly modulated in an aqueous solution, and that the signal can be readily extracted from a bright background using OLID. To further prove that Dasy makes an excellent candidate for contrast-enhancement in fluorescence microscopy, Paper I also includes measurements with Dasy(o) mixed with L929 cells. These results show that the amplitude modulated fluorescence of Dasy can be detected in a cellular environment with excellent fatigue resistance. Further details of the cell studies are given in Paper I.

5

All-visible-light switching of DAEs through triplet sensitization

Facilitating ring-closing reactions of DAEs generally require UV light, bringing drawbacks such as photodegradation and poor tissue penetration.[6,7] There are many examples of different approaches aiming at all-visible-light switching of DAEs.[52] One such approach has been to chemically extend the π conjugation requiring complicated synthesis,[53,54] while using upconverting nanoparticles to generate UV light from visible or near-IR light has lead to low photoisomerization quantum yields.[55,56] Another strategy has been to use TET from molecular triplet sensitizers,[22–25] but this approach also suffers from undesirable traits such as constrained molecular design, low molar absorptivities and high oxygen sensitivity. In this project, we propose a general approach with maintained high photoisomerization efficiencies and excellent fatigue resistance compared to direct UV isomerization.

Nanocrystals (NCs), or quantum dots are semiconducting and quantum confined inorganic crystals. They have several properties that makes them applicable in photochemical contexts,[57–59] such as high molar absorptivities and often stable and high photoluminescence quantum yields.[60] By varying the synthesis conditions such as temperature and time, the size of the NCs can be easily controlled.[61,62] Since the absorption and emission profiles are strongly dependent on the size of the NCs, they can be easily adapted to suit different energetic requirements. NCs display strong spin-orbit coupling, leading to such a small energy difference between the first singlet and triplet excited states that they can be considered as one. Although these are all appealing properties for triplet sensitizers they suffer from a very short triplet lifetime, which limits the use of NCs

as sensitizers in diffusion limited processes. Therefore, we attach phenanthrene-3-carboxylic acid (3-PCA) molecules to the surface of cadmium sulfide (CdS) NCs to act as triplet mediators by prolonging the triplet lifetime.[63–65] Schematic illustrations of the CdS NCs/3-PCA hybrids are shown both in Figure 5.1 and Figure 5.2 together with the molecular structure of 3-PCA.

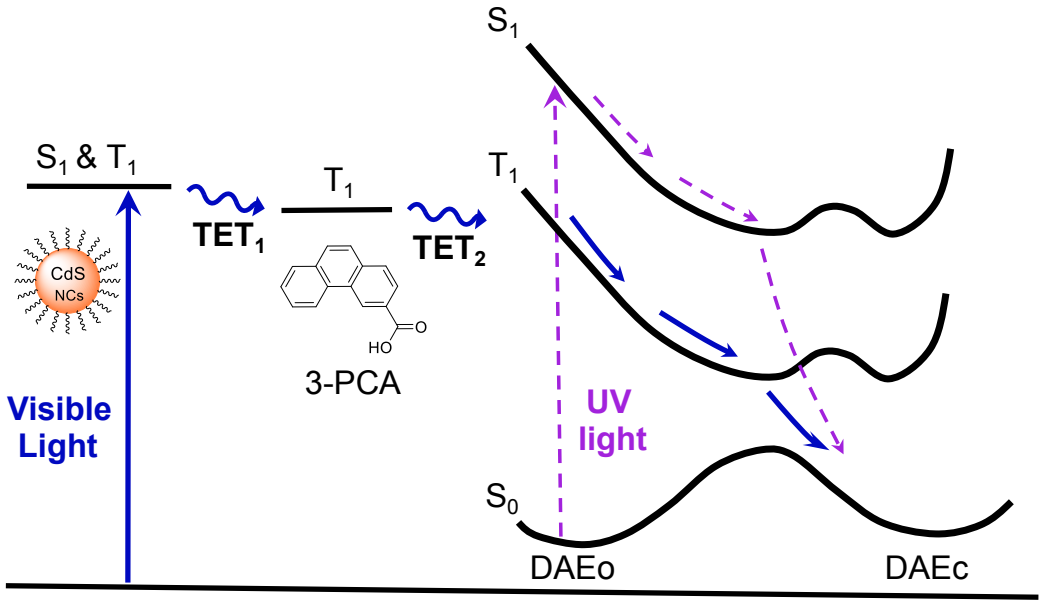

Figure 5.1: Schematic illustration showing the photoisomerization of DAEs, going from DAEo to DAEc. The route induced by visible light irradiation *via* two triplet energy transfer steps (TET_1 and TET_2) through CdS NCs and 3-PCA is shown as blue arrows, and direct UV induced isomerization is shown as dashed purple arrows.

The visible light isomerization from DAEo to DAEc using our CdS NCs/3-PCA hybrid triplet sensitizers is illustrated in Figure 5.1 as blue arrows. Visible light is used to excite the CdS NCs, and is followed by two triplet energy transfer steps (TET_1 and TET_2) first to 3-PCA and then to DAEo which results in isomerization to DAEc along the triplet manifold. As a comparison, direct UV isomerization along the singlet manifold of the DAE is shown as purple dashed arrows. To show the generality of our approach to all-visible-light isomerization of DAEs, we use four DAE derivatives referred to as DAE1, DAE2, DAE3 and DAE4. Their structures and isomerization schemes are shown in Figure 5.2. DAE1 and DAE2 are sensitized using CdS NCs with an absorption peak at 405 nm, hence the notation CdS 405 in the figure. The two other DAEs are sensitized using CdS NCs

with absorption peaks at 425 nm and 450 nm, and all CdS NCs are synthesized to match the desired irradiation wavelength used to induce the ring-closing reactions for the four DAEs (405 nm, 425 nm and 445 nm respectively for the three differently sized CdS NCs). 590 nm light is used to facilitate the reverse isomerization for all four DAEs.

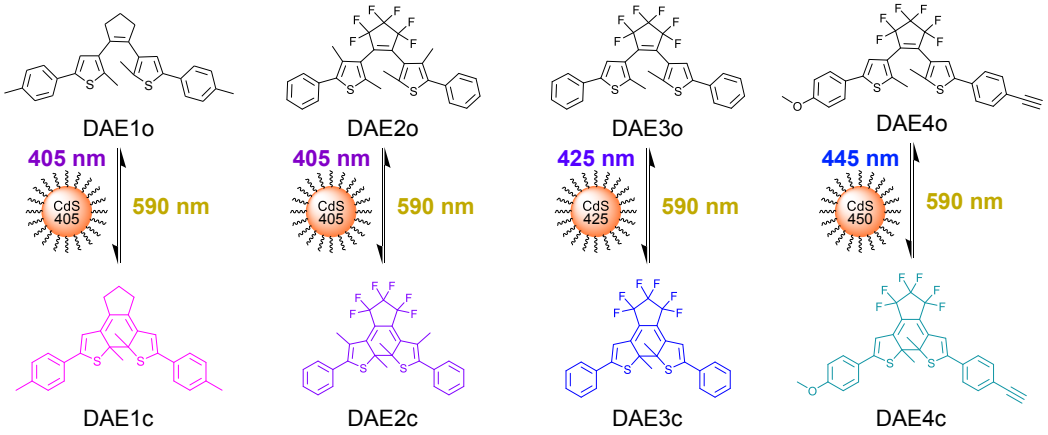

Figure 5.2: Structures and isomerization scheme of the four DAEs referred to as DAE1, DAE2, DAE3 and DAE4. CdS NCs with varying absorption bands are used to facilitate visible light (405 nm, 425 nm and 445 nm) induced isomerization from DAEo to DAEc, and 590 nm light is used to facilitate the reverse isomerization.

5.1 All-visible-light switching

To achieve all-visible-light switching of the DAEs and to ensure that it is indeed the TET that drives the photoisomerization, CdS NCs were synthesized according to previous reports[66,67] to have absorption bands that match the transparent windows of the photochromic molecules. 3-PCA was anchored to the CdS NC surface through its carboxylic acid functional groups, and the mediator is transparent for wavelengths longer than 370 nm meaning that it will not absorb any of the visible light sources used to induce the sensitized ring-closing reactions. 0.5 μM CdS was mixed with 100 μM 3-PCA hybrids and 50 μM of the respective DAEs in their open as-synthesized form into a 'cocktail'. Absorption spectra of the four DAEo mixtures in deareated toluene are shown in Figure 5.3 (black lines). Light matching the CdS NC absorption bands (405 nm for DAE1 and DAE2, 425 nm for DAE3 and 445 nm for DAE4) was then irradiated onto the samples, resulting in formation of DAEc (blue lines).

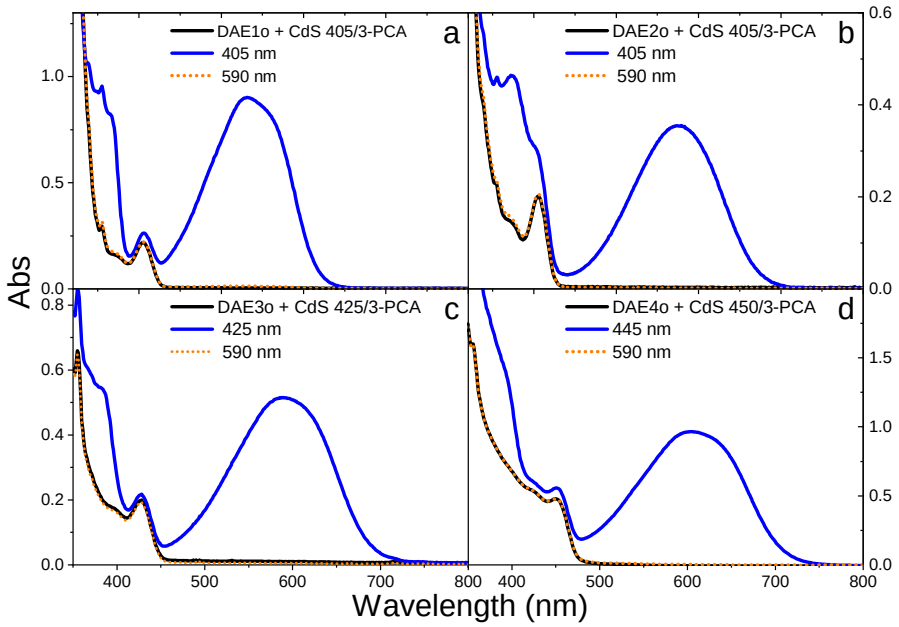

Figure 5.3: Absorption spectra of solutions containing the four DAE derivatives (50 μM of a) DAE1, b) DAE2, c) DAE3, and d) DAE4), CdS NCs (0.5 μM CdS 405 in a and b, 0.3 μM CdS 425 in c, and 0.5 μM CdS 450 in d) and 3-PCA (100 μM) in deareated toluene. Spectra are recorded for the open isomers before (black lines) and after irradiation of 405 nm, 425 nm, and 445 nm light respectively (120 s, blue lines), and then after 590 nm light irradiation (90 s, orange dotted lines).

At the PSS after 405 nm irradiation of the DAE1 sample, it reached a 94% conversion to the closed isomer (see Figure 5.3a) which is the same conversion that has been reported for UV irradiation.[30] The photocyclization quantum yield was also comparable to what has been reported for 313 nm UV light (35% in our case, compared to 43%[30]). The conversion of DAE2 using 405 nm light (see Figure 5.3b) was lower than what has previously been reported for 313 nm irradiation (58% vs 79%[68]), which we assign to the larger spectral overlap between DAE2c absorption and the excitation light. This overlap means that the triplet mediated ring-closing reaction competes with the direct ring-opening using the singlet manifold. The photocyclization quantum yield under 405 nm for the DAE2 cocktail on the other hand was comparable to 313 nm UV light isomerization (39% compared to previously reported 46%[68]). It is evident in Figures 5.3c and 5.3d that also DAE3 and DAE4 can be isomerized to their respective

closed form isomers using our approach. All four DAEs are then isomerized back to their open form isomers by 590 nm irradiation (orange dotted lines).

UV light triggers the formation of annulated byproducts of the DAEs.[29,30] This is evident when the absorbance at 530 nm of DAE1 was recorded over time (see Figure 5.4). The figure to the left shows the results of eight irradiation cycles of 405 nm and 590 nm light for the mixture of DAE1 and CdS 405/3-PCA hybrids (black), together with corresponding irradiation cycles using 302 nm and 590 nm light irradiation on DAE1 alone (red). It is evident that the fatigue resistance is better for the all-visible-light switching of the DAE1 mixture. Note that the lines connecting the measured absorbance values marked as squares are only there as a visual guide for the reader to easier follow the irradiation cycles. Another comparison showing the improved fatigue resistance when using visible instead of UV light can be seen in the Figure to the right. Here, the 530 nm absorbance of DAE1c is recorded over time starting with only DAE1o isomers in the samples. The mixture is irradiated with 405 nm light (black) and DAE1 alone is irradiated with 302 nm light (red).

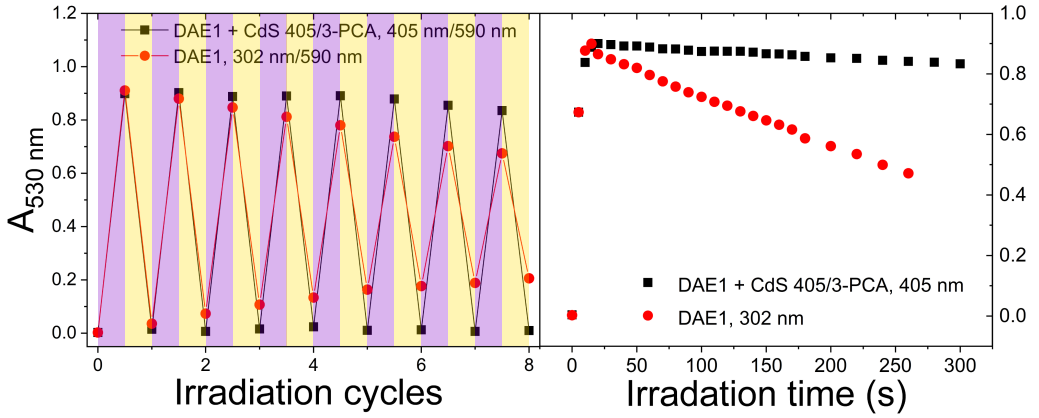

Figure 5.4: Absorbance of DAE1 at 530 nm. **Left:** recorded over eight irradiation cycles of 405 nm and 590 nm light for the DAE1 + CdS 405/3-PCA mixture (black), and for DAE1 alone using 302 nm and 590 nm light for the irradiation cycles (red). **Right:** recorded over time for the mixture irradiated with 405 nm light (black), and for DAE1 alone irradiated with 302 nm light (red). Both starting with DAE1o.

5.2 Investigation of the TET process

The TET_1 process from CdS 405 to 3-PCA was determined to have an efficiency close to unity (91%), and details on this determination are given in the Supporting Information of Paper II. Details on the triplet energies of the compounds are also given in this paper. A curious thing to note regarding the triplet energies is that although the triplet energy of DAE1o is estimated to be slightly lower than that of 3-PCA (2.5 eV[30] vs 2.6 eV[65]), the opposite is true for DAE2o which is estimated to have a triplet energy of 2.8 eV. According to Sandros equation, endothermic TET can still occur under these circumstances, although slower.[69]

Nanosecond transient absorption spectroscopy (ns-TA) was used to investigate the TET_2 process when adding DAE1 and DAE2 respectively to solutions containing 1.5 μM CdS 405 and an excess of 300 μM 3-PCA in deareated toluene to ensure formation of triplet excited 3-PCA through TET_1. A 415 nm pulsed laser (2.0 mJ, 10 ns) was used as the excitation source for the DAE1 measurement, and the DAE2 sample was excited with a 410 nm pulsed laser. The TA signal was recorded at 470 nm and 450 nm respectively for the DAE1 and DAE2 measurements (see Figure 5.5 top figures), both wavelengths within the broad positive absorption band of the 3-PCA triplet state.[65] Initially a rise in the TA signal can be seen in both figures, due to the formation of triplet excited 3-PCA. When no DAE derivatives are present, the triplet signal of 3-PCA then decays monoexponentially with a lifetime of 22 μs. This lifetime decreases when adding DAE1 and DAE2 respectively, since the 3-PCA triplet energy is now transferred to the DAE derivatives through TET_2. DAE1 and DAE2 can here be seen as triplet quenchers, and this effect can be investigated using the Stern-Volmer equation:

$$\frac{\tau_0}{\tau} = 1 + \tau_0 k_q [Q] \tag{5.1}$$

where τ_0 and τ are the triplet lifetimes in the absence and in the presence of DAE, respectively. k_q is the bimolecular quenching rate constant and [Q] is the quencher (i.e. DAE) concentration. Stern-Volmer plots are shown in the bottom part of Figure 5.5 for DAE1 (left) and DAE2 (right) together with their respective linear fits (red lines). The fitting resulted in k_q values of $1.4 \cdot 10^9$ $M^{-1}s^{-1}$ for DAE1 and $2.7 \cdot 10^7$ $M^{-1}s^{-1}$ for DAE2. The value for DAE1 is within the magnitude that

is expected for an efficient diffusion-controlled process, while the k_q for DAE2 is almost two orders of magnitude smaller. This is consistent with the previous discussion regarding the triplet energy of DAE2o being somewhat larger than that of 3-PCA resulting in a slower endothermic TET_2 process.

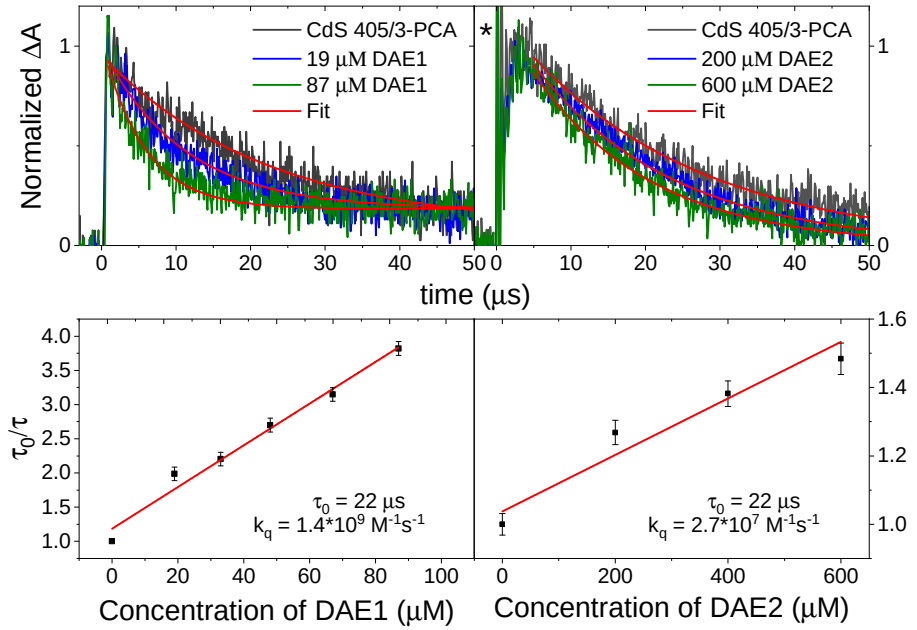

Figure 5.5: DAE quenching of the CdS 405/3-PCA hybrid triplet state. **Top figures:** Time-resolved transient absorption decays of CdS 405/3-PCA (1.5 μM CdS 405 and 300 μM 3-PCA) in deareated toluene, recorded at 470 nm upon 415 nm pulsed excitation adding DAE1 (left) and recorded at 450 nm upon 410 nm pulsed excitation adding DAE2 (right). *The initial rise in the DAE2 traces is due to laser scattering. **Bottom figures:** Stern-Volmer plots with linear fits (red lines) for DAE1 (left) and DAE2 (right) quenching of the CdS 405/3-PCA triplet lifetime.

5.3 Solid state switching

We have shown that our proposed system acts as a general approach to all-visible-light isomerization of a variety of DAE derivatives. The photoisomerization quantum yields are comparable to when isomerizing using UV light, and cyclization using the triplet manifold shows improved fatigue resistance. On top of this, Figure 5.6 shows that the CdS NCs/3-PCA hybrids perform well also in

the solid state. The solid state experiments were performed by soaking a filter paper in a solution containing CdS 405, 3-PCA and the colorless DAE2o in toluene and allowing the solvent to evaporate. Subsequent irradiation with 405 nm and 590 nm light and the use of masks induce color and pattern changes as seen in the figure, when switching the DAE2 between the colorless DAE2o and the colored DAE2c. More details are given in Paper II.

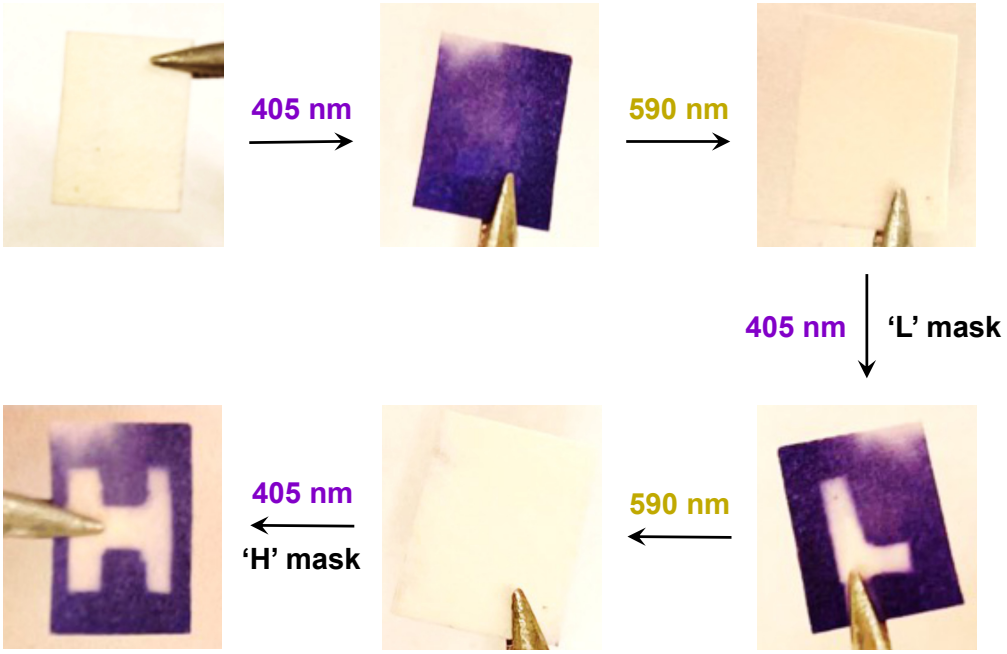

Figure 5.6: Photographs showing all-visible-light-switching of DAE2 in solid state. A filter paper was soaked in a solution containing DAE2, CdS 405 and 3-PCA. After solvent evaporation, the color (white and purple) and pattern (letters 'L' and 'H') were changed by subsequently irradiating the filter paper with 405 nm and 590 nm light. This was all done in a normal atmospheric environment.

6

DAE isomerization using triplet-triplet annihilation photon upconversion

In the previous chapter, isomerization using triplet sensitization allowed the use of visible light to facilitate ring-closing reactions for DAEs that typically require UV light. A drawback with using triplet sensitization to drive photochemical reactions is that TET requires the sensitizer to be in close proximity to the photochemical reactant.[22–25] This is not a problem if no further separation step of the sensitizer and the photochemical products is required and the two components are in the same phase (such as the liquid solutions used in the previous chapter). Here, we instead use TTA-PUC[11] to facilitate isomerization of DAEs using light with lower energy than absorbed by the photoswitch which allows us to keep the upconversion (UC) solution and the DAE solution physically separated. TTA-PUC have previously been used to facilitate various types of photochemical reactions,[38,70–78] including photoisomerization.[79]

In this project, we use a single green light source to both drive the reversible isomerization and induce fluorescence from the closed isomer of a group of DAE derivatives. Results using the derivative referred to in Paper III as DAE2 (note that this is another DAE derivative than the one referred to as DAE2 in Chapter 5) will be shown in this chapter, while the reader is referred to the paper for details on the other two DAEs. Both the ring-opening reaction and inducing fluorescence from DAE2c can be directly controlled using green light, but the ring-closing reaction requires higher energy light (typically in the UV region). To drive also this latter process using our green light source, we use a well studied

green-to-blue TTA-PUC pair consisting of platinum octaethylporphyrin (PtOEP) as the sensitizer and 9,10-diphenylanthracene (DPA) as the annihilator. The upconverted blue light has sufficiently high energy to facilitate the ring-closing reaction. Molecular structures of PtOEP and DPA can be seen in the top panel of Figure 6.1, and the structures and isomerization scheme between DAE2o and DAE2c are seen in the bottom panel of this figure.

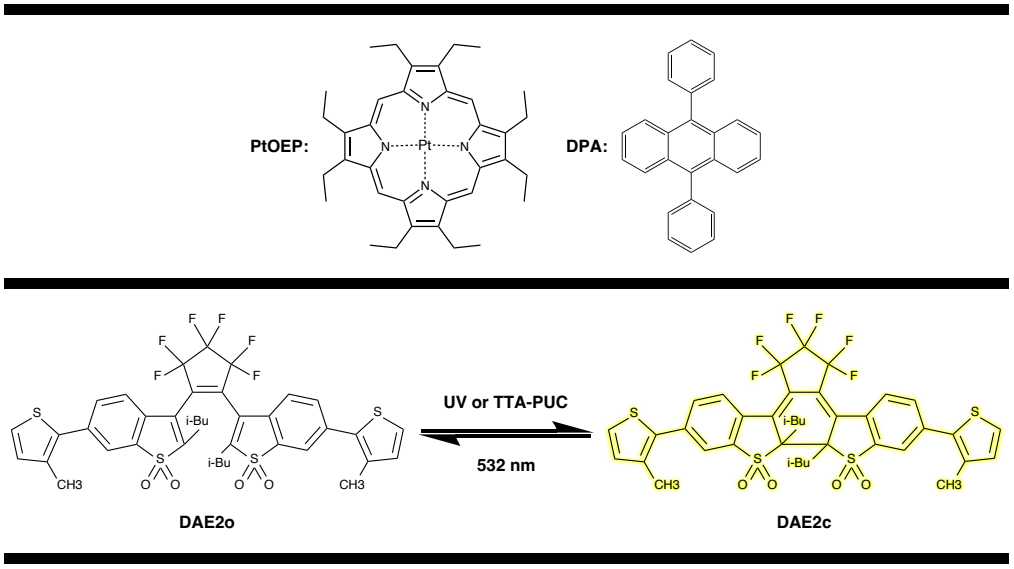

Figure 6.1: Top panel: PtOEP and DPA structures. **Bottom panel:** Structures and isomerization scheme of DAE2. 365 nm UV light or upconverted (TTA-PUC) light can be used to isomerize from DAE2o to DAE2c, and 532 nm light is used to facilitate the reverse isomerization. The yellow glow on DAE2c is there to visualize its green light induced fluorescence.

The DAE2 solution and the UC solution are kept physically separated in a two-chamber quartz cuvette, as shown in the photographs in Figure 6.2. When driving the isomerization from DAE2c to DAE2o, 532 nm light is irradiated only through the DAE2 cuvette. The rightmost photograph shows the laser irradiation (visualized by a green arrow) when instead starting with DAE2o in the DAE2 chamber and driving the ring-closing reaction and subsequently triggering the fluorescence of DAE2c. During this experiment, the laser is irradiated through the DAE2 chamber that at time zero does not absorb any of the incoming 532 nm laser light. The green light then reaches the UC chamber, which was prepared with concentrations (10 mM DPA and 0.5 mM PtOEP in toluene)

that ensure 99% attenuation of the 532 nm light within the first millimeter of the UC chamber. This was done so that most of the TTA-PUC occurs close to the quartz wall separating the two solutions, and the short distance back to the DAE2 chamber results in minimized secondary inner-filter effects of the blue UC fluorescence before reaching the photochromic molecules.

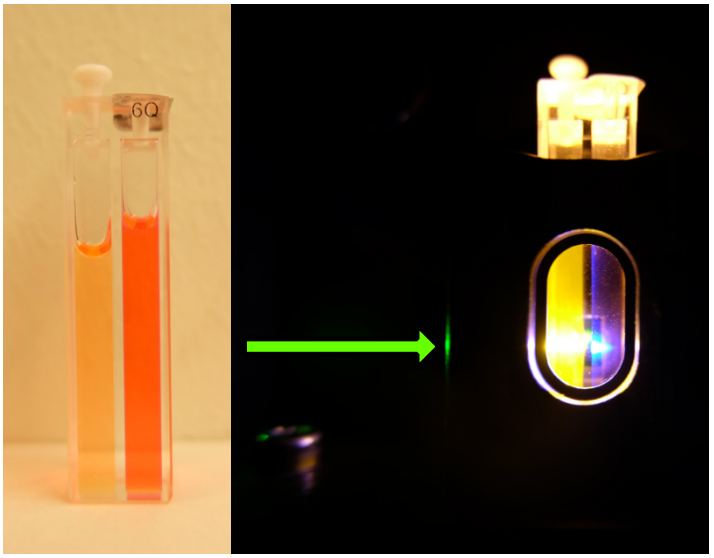

Figure 6.2: Photographs showing two-chamber cuvettes containing DAE2 (left chamber) and PtOEP/DPA upconversion solution (right chamber), both in toluene. The photograph to the left shows the cuvette in ambient light, and the photograph to the right shows the cuvette in the dark during 532 nm laser irradiation from the left (indicated by the green arrow) through the DAE2 chamber into the upconversion chamber.

Absorption spectra of DAE2o and DAE2c are shown in Figure 6.3, together with normalized DAE2c fluorescence and upconverted DPA emission measured semi-front-face in the two-chamber cuvette (see Paper III for measurement details). As for the DAE derivatives presented in the previous chapters, DAE2o mainly absorb UV light while DAEc also displays absorption in the visible region. DAE2c is strongly fluorescent with a fluorescence quantum yield of 0.83, and its yellow fluorescence can be seen also in the rightmost photograph in Figure 6.2. There is a small spectral overlap of the DAE2o absorption and the upconverted emission (see Figure 6.3), which enables the use of upconverted photons to drive the ring-closing reaction. It is evident that there is a larger spectral overlap between the upconverted emission and the DAEc absorption, which would mean that also the ring-opening reaction should be triggered by our TTA-PUC. The reason to why

we can still drive isomerization from DAE2o to DAE2c is that the isomerization quantum yield of the ring-closing reaction (0.39) is several orders of magnitude larger than that of the ring-opening reaction ($2.4{\cdot}10^{-4}$) for this derivative.

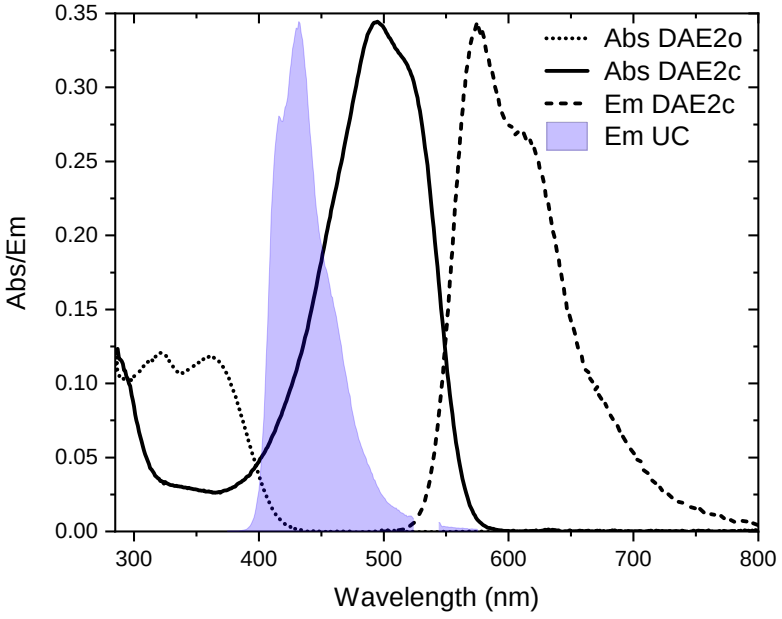

Figure 6.3: Absorption spectra of DAE2o (dotted black line) and DAE2c (solid black line) together with the emission spectra of DAE2c (dashed black line) and the upconverted DPA emission as measured in the two-chamber cuvette setup (purple filled). All spectra are measured in toluene, and the upconversion sample was prepared in an oxygen free environment.

6.1 Green light control of reversible DAE isomerization and fluorescence

Emission readout of the DAE2c fluorescence was used to show that TTA-PUC can be used to trigger the ring-closing reaction. Figure 6.4 shows the time-profile of the DAE2c fluorescence measured at its emission maximum in toluene (578 nm). At the start of the measurement, DAE2 was in its as-synthesized non-fluorescent open form. A 532 nm laser was turned on at time zero, resulting in an immediate rise in the emission signal when there was UC solution present in the other cuvette chamber (black) and no significant emission signal with only

toluene in the other cuvette chamber (orange). This difference clearly shows that the green-to-blue upconversion triggers the ring-closing reaction. With time, the intensity of the fluorescence levels out at the PSS resulting from the DAE2 chamber being simultaneously subjected to 532 nm irradiation and upconverted photons.

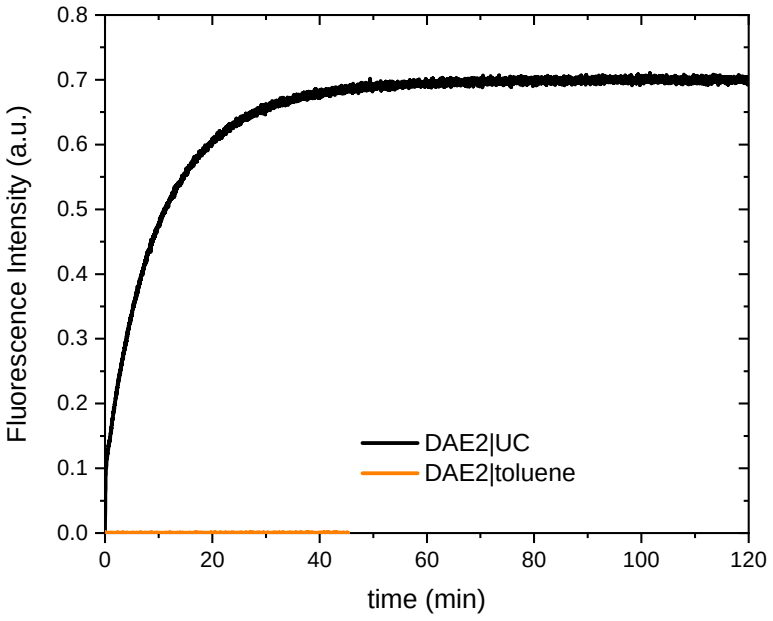

Figure 6.4: DAE2c fluorescence measured at its emission peak at 578 nm over time, measured in the two-chamber cuvette with (black) and without (orange) upconversion solution in the other cuvette chamber. Initially, the DAE chamber contained only the non-fluorescent DAE2o isomer. At time zero the 532 nm laser was turned on, resulting in DAEc formation and subsequent fluorescence in the presence of upconversion solution. In the absence of upconversion solution, no significant DAEc fluorescence was detected indicating that no DAEc was formed.

Our two-chamber cuvette setup allows us to chose what photophysical process will be triggered by the 532 nm laser simply by irradiating different parts of the cuvette. In Figure 6.5, only the DAE2 chamber was irradiated. At time zero, DAE2 was in its closed isomeric form displaying strong absorption at 532 nm. Absorption spectra resulting from 1, 3 and 5 hours of 532 nm irradiation are shown together with spectra of DAE2o and DAE2c. It is clear that also the DA2c to DAE2o isomerization can be triggered by the same light source used to trigger

the ring-closing reaction and inducing fluorescence of DAE2c, and after 5 hours almost all DAE2c have isomerized to DAE2o.

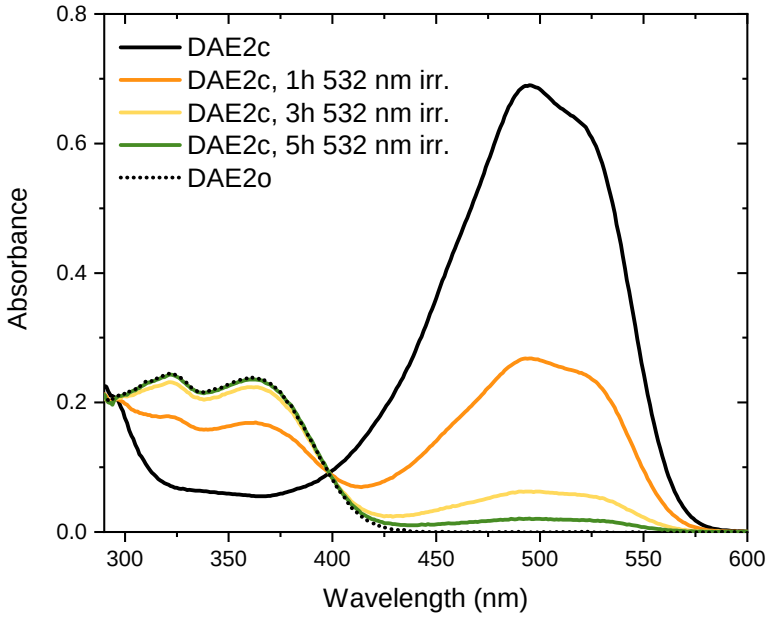

Figure 6.5: Absorption spectra of DAE2c (solid black line) and DAE2o (dotted black line), together with the resulting spectra of DAE2c after 1 (orange line), 3 (yellow line) and 5 (green line) hours of 532 nm laser irradiation only through the DAE2 chamber. Hence, no TTA-PUC occurred and therefore only the ring-opening reaction was triggered by the green light.

6.2 Performance of the TTA-PUC driven isomerization

Last, the performance of the TTA-PUC driven isomerization from DAE2o to DAE2c was compared to direct 365 nm LED driven isomerization (see Figure 6.6). This was done by preparing highly concentrated (approximately 800 μM) DAE2 solutions in one cuvette chamber, and filling the other chamber with either UC solution or toluene. Further details regarding this comparison are presented in Paper III, but in short the high concentration of DAE2 allowed for the approximation of total absorption of the upconverted and the 365 nm photons. Linear fitting of the initial 0^{th} order kinetics together with the difference in irradiation power of the two light sources (16.2 mW for the 532 nm laser and 0.21 mW for the 365 nm LED), indicated that the direct 365 nm LED driven isomerization was

140 times more efficient than the TTA-PUC driven isomerization. This difference can be explained by loss factors such as the poor spectral overlap of the DAE2o absorption and the upconverted emission, the angular spread of upconverted photons, and the upconversion efficiency which were estimated to have efficiencies of 24%, 50% and 6%, respectively in our setup. By further optimization of the proposed system, most of these loss factors could be minimized.

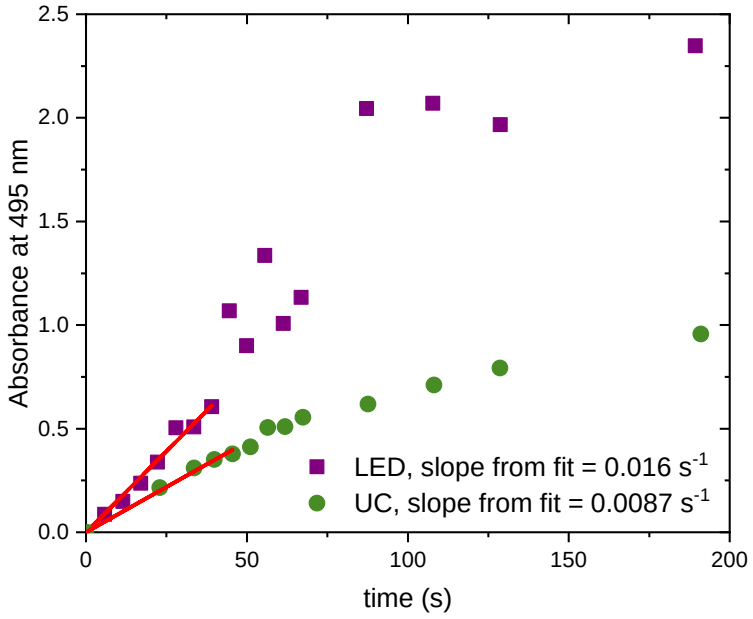

Figure 6.6: Comparison of the absorbance at the 495 nm centered DAE2c peak recorded over time during isomerization from DAE2o when using either a 365 nm LED (purple squares) or TTA-PUC (green circles), together with linear fits (red lines) of the initial absorbance change.

From this study, it is evident that a single green light source can be used to facilitate both reversible photoisomerization of three DAE derivatives and induce fluorescence of DAEc by using green-to-blue TTA-PUC. This was done in a simple and versatile experimental setup, in which the triggered process can be selected by simply irradiating different parts of the sample. The physical separation of the UC and the DAE solution enables characterization of the two solutions both individually and in synchrony. Another advantage of the physical separation is that there is no need for further separation procedures, and concentrations and solvents can be easily adjusted individually for the two cuvette chambers.

7

Conclusion and Outlook

The objective of this thesis spans over three comprehensive studies on different ways of modulating diarylethene photoswitches. Although the approaches in the three included papers are different, they all present examples on how to manipulate light to match our needs. By modulating DAEs using the presented unconventional methods we have shown that visible light can be used to control photophysical processes that typically require UV light, such as UV triggered photoisomerization and fluorescence.

In Paper I, it was shown that fluorescence of the water-soluble DAE derivative Dasy could be rapidly modulated using red light. With modulation frequencies reaching 205 Hz, this strongly exceeds previous reports of less than 1 Hz. The modulated fluorescence could easily be distinguished from a bright background using optical lock-in detection, and the rapid modulation could also be detected in a cellular environment using fluorescence microscopy. These results show that Dasy is an excellent candidate for contrast-enhanced fluorescence microscopy, where the next step would be to combine the lock-in interfaced detection with a microscope.

Paper II focuses on all-visible-light switching of a group of DAE derivatives, by using CdS NC/3-PCA hybrids to isomerize the DAEs using the triplet manifold instead of using direct UV isomerization. Since the absorption bands of the CdS NCs can be shifted to match different wavelengths by simple synthesis measures, this is shown to be a versatile approach. Isomerization using TET improved the fatigue resistance of the DAEs, while maintaining comparable isomerization quantum yields to using UV light. Some future steps could be to gain deeper tissue penetration by applying two-photon absorption, coating the CdS NCs with

nontoxic organic molecules or polymers or functionalizing DAE derivatives with carboxylic acid functional groups to remove the need of mediators.

The work in Paper III also focuses on all-visible-light control of DAEs, by the use of TTA-PUC to achieve single wavelength control of both reversible photoisomerization and fluorescence of yet another group of DAEs. TTA-PUC allows for physical separation of the upconversion and the DAE solution, which would be a requirement in future applications where solid state TTA-PUC is thought to be used. The proposed setup was not very efficient compared to direct UV isomerization, but the simplicity and versatility of the setup allowed for *in situ* characterization of the photoisomerization, teaching us about combining TTA-PUC and photochemical reactions. Hence, this paper can be seen more as a proof-of-concept study and a way to understand the processes relevant when using TTA-PUC to facilitate high energy photochemical reactions using e.g. the abundant visible sunlight in solar fuel production.

Overall, the work presented in this thesis has shown how factors like tissue penetration, photodegradation and future possibilities to use visible light in applications that typically require UV light can be improved by modulating and manipulating light to fit the application at hand. Further optimization and mechanistic understanding is needed for these methods to reach their full potential, and with the findings presented in this thesis a few more steps towards visble-light control of high energy photochemical transformations has been taken.

8

Acknowledgements

This work would not have been half as good or enjoyable without the help and support from the people around me - thank you for that! I especially would like to mention some of you:

My supervisor Bo Albinsson: I very much appreciate your view on research and your eagerness to teach and guide me in my studies. Also my co-supervisor Joakim Andréasson for being very involved in all of my research projects, and always ready to discuss chemistry. I think the two of you make the best supervisory team I could ever have asked for!

Jerker Mårtensson who has followed my learning journey both as my examiner and line manager, the latter also includes Nina Kann. Gaowa and Lili: thank you for all our time in the lab working on our shared projects. I have learnt a lot from both of you! Thank you also to Fredrik, Andrew, Axel, Carlos and Liam for proofreading this thesis, and thank you to Deise and Rasmus for agreeing to be opponents during the seminar.

My wonderful office mates Jesper and Fredrik - thank you for being you and for making me feel welcome from my very first day! The past and current group meeting members from the extended Abrahamsson, Albinsson and Andréasson research groups for all the interesting discussions and support. And thank you to all the people on floor five for the great atmosphere at work.

Last but not least my dear family and friends who always support me!

Wera Larsson, Gothenburg, SEPTEMBER 2022

Bibliography

[1] N. S. Lewis and D. G. Nocera. Powering the planet: Chemical challenges in solar energy utilization. *Proceedings of the National Academy of Sciences*, 103(43):15729–15735, 2006.

[2] C. Kittel. *Introduction to Solid State Physics*. John Wiley & Sons, Inc, New York, USA, eighth edition, 2005.

[3] W. Shockley and H. J. Queisser. Detailed Balance Limit of Efficiency of p-n Junction Solar Cells. *Journal of Applied Physics*, 32(3):510–519, 1961.

[4] A. Fujishima and K. Honda. Electrochemical Photolysis of Water at a Semiconductor Electrode. *Nature*, 238:37–38, 1972.

[5] A. J. Bard and M. A. Fox. Artificial Photosynthesis: Solar Splitting of Water to Hydrogen and Oxygen. *Accounts of Chemical Research*, 28(3):141–145, 1994.

[6] W. A. Velema, W. Szymanski, and B. L. Feringa. Photopharmacology: beyond proof of principle. *Journal of the American Chemical Society*, 136(6):2178–2191, 2014.

[7] J. Broichhagen, J. A. Frank, and D. Trauner. A roadmap to success in photopharmacology. *Account of Chemical Research*, 48(7):1947–1960, 2015.

[8] M. Irie. Diarylethenes for Memories and Switches. *Chemical Reviews*, 100(5):1685–1716, 2000.

[9] H. Tian and S. Yang. Recent progresses on diarylethene based photochromic switches. *Chemical Society Reviews*, 33(2):85–97, 2004.

[10] M. Irie, T. Fukaminato, K. Matsuda, and S. Kobatake. Photochromism of Diarylethene Molecules and Crystals: Memories, Switches, and Actuators. *Chemical Reviews*, 114(24):12174–12277, 2014.

[11] T. N. Singh-Rachford and F. N. Castellano. Photon upconversion based on sensitized triplet–triplet annihilation. *Coordination Chemistry Reviews*,

254(21-22):2560–2573, 2010.

[12] J. M. Hollas. *Modern Spectroscopy*. John Wiley & Sons, Chichester, England, fourth edition, 2004.

[13] T. Förster. Zwischenmolekulare Energiewanderung und Fluoreszenz. *Annalen der Physik*, 437(1-2):55–75, 1948.

[14] D. L. Dexter. a theory of sensitized luminescence in solids.

[15] M. Irie. *Diarylethene Molecular Photoswitches: Concepts and Functionalities*. Wiley-VCH, Weinheim, Germany, first edition, 2021.

[16] T. Leydecker, M. Herder, E. Pavlica, G. Bratina, S. Hecht, E. Orgiu, and P. Samori. Flexible non-volatile optical memory thin-film transistor device with over 256 distinct levels based on an organic bicomponent blend. *Nature Nanotechnology*, 11(9):769–775, 2016.

[17] L. Hou, X. Zhang, G. F. Cotella, G. Carnicella, M. Herder, B. M. Schmidt, M. Patzel, S. Hecht, F. Cacialli, and P. Samori. Optically switchable organic light-emitting transistors. *Nature Nanotechnology*, 14(4):347–353, 2019.

[18] Y. Zou, T. Yi, S. Xiao, F. Li, C. Li, X. Gao, J. Wu, M. Yu, and C. Huang. Amphiphilic Diarylethene as a Photoswitchable Probe for Imaging Living Cells. *Journal of the American Chemical Society*, 130(4):15750–15751, 2008.

[19] K. Uno, M. L. Bossi, V. N. Belov, M. Irie, and S. W. Hell. Multicolour fluorescent "sulfide-sulfone" diarylethenes with high photo-fatigue resistance. *Chemical Communications*, 56(14):2198–2201, 2020.

[20] G. S. Hammond, N. J. Turro, and P. A. Leermakers. The Mechanisms of Photoreactions in Solution. IX. Energy Transfer From the Triplet States of Aldehydes and Ketones to Unsaturated Compounds. *Journal of Physical Chemistry*, 66(6):1144–1147, 1962.

[21] L. D. Elliott, S. Kayal, M. W. George, and K. Booker-Milburn. Rational Design of Triplet Sensitizers for the Transfer of Excited State Photochemistry from UV to Visible. *Journal of the American Chemical Society*, 142(35):14947–14956, 2020.

[22] R. T. F. Jukes, V. Adamo, F. Hartl, P. Belser, and L. De Cola. Photochromic Dithienylethene Derivatives Containing Ru(II) or Os(II) Metal Units. Sensitized Photocyclization from a Triplet State. *Inorganic Chemistry*, 43(9):2779–2792, 2004.

[23] V. W.-W. Yam, C.-C. Ko, and N. Zhu. Photochromic and Luminescence Switching Properties of a Versatile Diarylethene-Containing 1,10-Phenanthroline Ligand and Its Rhenium(I) Complex. *Journal of the American Chemical Society*, 126(40):12734–12735, 2004.

[24] S. Fredrich, R. Gostl, M. Herder, L. Grubert, and S. Hecht. Switching Diarylethenes Reliably in Both Directions with Visible Light. *Angewandte Chemie, International Edition*, 55(3):1208–1212, 2016.

[25] Z. Zhang, W. Wang, P. Jin, J. Xue, L. Sun, J. Huang, J. Zhang, and H. Tian. A building-block design for enhanced visible-light switching of diarylethenes. *Nature Communications*, 10(1):4232, 2019.

[26] C. Grewer and H.-D. Brauer. Mechanism of the Triplet-State Quenching by Molecular Oxygen in Solution. *Journal of Physical Chemistry*, 98(16):4230–4235, 1994.

[27] C. G. Hübner, A. Renn, I. Renge, and U. P. Wild. Direct observation of the triplet lifetime quenching of single dye molecules by molecular oxygen. *The Journal of Chemical Physics*, 115(21):9619–9622, 2001.

[28] C. Schweitzer and R. Schmidt. Physical Mechanisms of Generation and Deactivation of Singlet Oxygen. *Chemical Reviews*, 103(5):1685–1758, 2003.

[29] M. Irie, T. Lifka, K. Uchida, S. Kobatake, and Y. Shindo. Fatigue resistant properties of photochromic dithienylethenes: by-product formation. *Chemical Communications*, (8):747–750, 1999.

[30] M. Herder, B. M. Schmidt, L. Grubert, M. Pätzel, J. Schwarz, and S. Hecht. Improving the Fatigue Resistance of Diarylethene Switches. *Journal of the American Chemical Society*, 137(7):2738–2747, 2015.

[31] Y. Zhou, F. N. Castellano, T. W. Schmidt, and K. Hanson. On the Quantum Yield of Photon Upconversion via Triplet–Triplet Annihilation. *ACS Energy Letters*, 5(7):2322–2326, 2020.

[32] W. Sun, A. Ronchi, T. Zhao, J. Han, A. Monguzzi, and P. Duan. Highly efficient photon upconversion based on triplet–triplet annihilation from bichromophoric annihilators. *Journal of Materials Chemistry C*, 9(40):14201–14208, 2021.

[33] A. Olesund, J. Johnsson, F. Edhborg, S. Ghasemi, K. Moth-Poulsen, and B. Albinsson. Approaching the Spin-Statistical Limit in Visible-to-

Ultraviolet Photon Upconversion. *Journal of the American Chemical Society*, 144(8):3706–3716, 2022.

[34] P. Gibart, F. Auzel, J.-C. Guillaume, and K. Zahraman. Below Band-Gap IR Response of Substrate-Free GaAs Solar Cells Using Two-Photon Up-Conversion. *Japanese Journal of Applied Physics*, 35(Part 1, No. 8):4401–4402, 1996.

[35] T. Trupke, M. A. Green, and P. Würfel. Improving solar cell efficiencies by up-conversion of sub-band-gap light. *Journal of Applied Physics*, 92(7):4117–4122, 2002.

[36] T. Trupke, A. Shalav, B. S. Richards, P. Würfel, and M. A. Green. Efficiency enhancement of solar cells by luminescent up-conversion of sunlight. *Solar Energy Materials and Solar Cells*, 90(18-19):3327–3338, 2006.

[37] Y. Y. Cheng, B. Fückel, R. W. MacQueen, T. Khoury, R. G. C. R. Clady, T. F. Schulze, N. J. Ekins-Daukes, M. J. Crossley, B. Stannowski, K. Lips, and T. W. Schmidt. Improving the light-harvesting of amorphous silicon solar cells with photochemical upconversion. *Energy & Environmental Science*, 5(5), 2012.

[38] K. Börjesson, D. Dzebo, B. Albinsson, and K. Moth-Poulsen. Photon upconversion facilitated molecular solar energy storage. *Journal of Materials Chemistry A*, 1(30):8521–8524, 2013.

[39] S. Baluschev, T. Miteva, V. Yakutkin, G. Nelles, A. Yasuda, and G. Wegner. Up-Conversion Fluorescence: Noncoherent Excitation by Sunlight. *Physical Review Letters*, 97(14):143903, 2006.

[40] R. R. Islangulov, J. Lott, C. Weder, and F. N. Castellano. Noncoherent Low-Power Upconversion in Solid Polymer Films. *Journal of the American Chemical Society*, 129(42):12652–12653, 2007.

[41] A. Haefele, J. Blumhoff, R. S. Khnayzer, and F. N. Castellano. Getting to the (Square) Root of the Problem: How to Make Noncoherent Pumped Upconversion Linear. *The Journal of Physical Chemistry Letters*, 3(3):299–303, 2012.

[42] J. R. Lakowicz. *Principles of Fluorescence Spectroscopy*. Springer, Baltimore, Maryland, USA, third edition, 2006.

[43] G. Naren, S. Li, and J. Andréasson. A simplicity-guided cocktail approach toward multicolor fluorescent systems. *Chemical Communications*,

56(23):3377–3380, 2020.

[44] K. Shibata, L. Kuroki, T. Fukaminato, and M. Irie. Fluorescence Switching of a Diarylethene Derivative Having Oxazole Rings. *Chemistry Letters*, 37(8):832–833, 2008.

[45] G. Marriott, S. Mao, T. Sakata, J. Ran, D. K. Jackson, C. Petchprayoon, T. J. Gomez, E. Warp, O. Tulyathan, H. L. Aaron, E. Y. Isacoff, and Y. Yan. Optical lock-in detection imaging microscopy for contrast-enhanced imaging in living cells. *Proceedings of the National Academy of Sciences of the United States of America*, 105(46):17789–17794, 2008.

[46] A. E. Keirstead, J. W. Bridgewater, Y. Terazono, G. Kodis, S. D. Straight, P. A. Liddell, A. L. Moore, T. A. Moore, and D. Gust. Photochemical "Triode" Molecular Signal Transducer. *Journal of the American Chemical Society*, 132(18):6588–6595, 2010.

[47] G. Copley, J. G. Gillmore, J. Crisman, G. Kodis, C. L. Gray, B. R. Cherry, B. D. Sherman, P. A. Liddell, M. M. Paquette, L. Kelbauskas, N. L. Frank, A. L. Moore, T. A. Moore, and D. Gust. Modulating Short Wavelength Fluorescence with Long Wavelength Light. *Journal of the American Chemical Society*, 136(34):11994–12003, 2014.

[48] S. Mao, R. K. Benninger, Y. Yan, C. Petchprayoon, D. Jackson, C. J. Easley, D. W. Piston, and G. Marriott. Optical Lock-In Detection of FRET Using Synthetic and Genetically Encoded Optical Switches. *Biophysical Journal*, 94(11):4515–4524, 2008.

[49] Z. Tian, W. Wu, W. Wan, and A. D. Li. Photoswitching-induced frequency-locked donor-acceptor fluorescence double modulations identify the target analyte in complex environments. *Journal of the American Chemical Society*, 133(40):16092–16100, 2011.

[50] L. Wu, Y. Dai, X. Jiang, C. Petchprayoon, J. E. Lee, T. Jiang, Y. Yan, and G. Marriott. High-contrast fluorescence imaging in fixed and living cells using optimized optical switches. *PLoS One*, 8(6):e64738, 2013.

[51] J. R. Nilsson, S. Li, B. Önfelt, and J. Andreasson. Light-induced cytotoxicity of a photochromic spiropyran. *Chemical Communications*, 47(39):11020–11022, 2011.

[52] D. Bleger and S. Hecht. Visible-Light-Activated Molecular Switches. *Angewandte Chemie International Edition*, 54(39):11338–11349, 2015.

[53] G. M. Tsivgoulis and J.-M. Lehn. Multiplexing optical systems: Multicolor-bifluorescent-biredox photochromic mixtures. *Advanced Materials*, 9(8):627–630, 1997.

[54] T. Fukaminato, T. Hirose, T. Doi, M. Hazama, K. Matsuda, and M. Irie. Molecular Design Strategy toward Diarylethenes That Photoswitch with Visible Light. *Journal of the American Chemical Society*, 136(49):17145–17154, 2014.

[55] J.-C. Boyer, C.-J. Carling, B. D. Gates, and N. R. Branda. Two-Way Photoswitching Using One Type of Near-Infrared Light, Upconverting Nanoparticles, and Changing Only the Light Intensity. *Journal of the American Chemical Society*, 132(44):15766–15772, 2010.

[56] T. Wu and N. R. Branda. Using low-energy near infrared light and upconverting nanoparticles to trigger photoreactions within supramolecular assemblies. *Chemical Communications*, 52(56):8636–8644, 2016.

[57] X. Michalet, F. F. Pinaud, L. A. Bentolila, J. M. Tsay, S. Doose, J. J. Li, G. Sundaresan, A. M. Wu, S. S. Gambhir, and S. Weiss. Quantum Dots for Live Cells, in Vivo Imaging, and Diagnostics. *Science*, 307(5709):538–544, 2005.

[58] Q. Sun, Y. A. Wang, L. S. Li, D. Wang, T. Zhu, J. Xu, C. Yang, and Y. Li. Bright, multicoloured light-emitting diodes based on quantum dots. *Nature Photonics*, 1(12):717–722, 2007.

[59] X. Dai, Z. Zhang, Y. Jin, Y. Niu, H. Cao, X. Liang, L. Chen, J. Wang, and X. Peng. Solution-processed, high-performance light-emitting diodes based on quantum dots. *Nature*, 515(7525):96–99, 2014.

[60] A. P. Alivisatos. Semiconductor Clusters, Nanocrystals, and Quantum Dots. *Science*, 271(5251):933–937, 1996.

[61] R. Rossetti, S. Nakahara, and L. E. Brus. Quantum size effects in the redox potentials, resonance Raman spectra, and electronic spectra of CdS crystallites in aqueous solution. *The Journal of Chemical Physics*, 79(2):1086–1088, 1983.

[62] X. Wang, J. Zhuang, Q. Peng, and Y. Li. A general strategy for nanocrystal synthesis. *Nature*, 437(7055):121–124, 2005.

[63] N. J. Thompson, M. W. B. Wilson, D. N. Congreve, P. R. Brown, J. M. Scherer, T. Bischof, M. Wu, N. Geva, M. Welborn, T. V. Voorhis, V. Bulović,

M. G. Bawendi, and M. Baldo. Energy harvesting of non-emissive triplet excitons in tetracene by emissive PbS nanocrystals. *Nature Materials*, 13(11):1039–1043, 2014.

[64] C. Mongin, S. Garakyaraghi, N. Razgoniaeva, M. Zamkov, and F. N. Castellano. Direct observation of triplet energy transfer from semiconductor nanocrystals. *Science*, 351(6271):369–372, 2016.

[65] L. Hou, A. Olesund, S. Thurakkal, X. Zhang, and B. Albinsson. Efficient Visible-to-UV Photon Upconversion Systems Based on CdS Nanocrystals Modified with Triplet Energy Mediators. *Advanced Functional Materials*, 31(47):2106198, 2021.

[66] W. W. Yu and X. Peng. Formation of High-Quality CdS and Other II–VI Semiconductor Nanocrystals in Noncoordinating Solvents: Tunable Reactivity of Monomers. *Angewandte Chemie, International Edition*, 41(13):2368–2371, 2002.

[67] Z. Li, Y. Ji, R. Xie, S. Y. Grisham, and X. Peng. Correlation of CdS Nanocrystal Formation with Elemental Sulfur Activation and Its Implication in Synthetic Development. *Journal of the American Chemical Society*, 133(43):17248–17256, 2011.

[68] M. Irie, K. Sakemura, M. Okinaka, and K. Uchida. Photochromism of Dithienylethenes with Electron-Donating Substituents. *The Journal of Organic Chemistry*, 60(25):8305–8309, 1995.

[69] K. Sandros. Transfer of Triplet State Energy in Fluid Solutions. III. Reversible Energy Transfer. *Acta Chemca Scandinavia*, 18:2355–2374, 1964.

[70] R. R. Islangulov and F. N. Castellano. Photochemical Upconversion: Anthracene Dimerization Sensitized to Visible Light by a RuII Chromophore. *Angewandte Chemie, International Edition*, 45(36):5957–5959, 2006.

[71] R. S. Khnayzer, J. Blumhoff, J. A. Harrington, A. Haefele, F. Deng, and F. N. Castellano. Upconversion-powered photoelectrochemistry. *Chemical Communications*, 48(2):209–211, 2012.

[72] S. H. Askes, A. Bahreman, and S. Bonnet. Activation of a photodissociative ruthenium complex by triplet-triplet annihilation upconversion in liposomes. *Angewandte Chemie, International Edition*, 53(4):1029–1033, 2014.

[73] O. S. Kwon, J. H. Kim, J. K. Cho, and J. H. Kim. Triplet-triplet annihilation upconversion in CdS-decorated SiO2 nanocapsules for sub-bandgap

photocatalysis. *ACS Applied Materials & Interfaces*, 7(1):318–325, 2015.

[74] M. Majek, U. Faltermeier, B. Dick, R. Perez-Ruiz, and A. Jacobi von Wangelin. Application of Visible-to-UV Photon Upconversion to Photoredox Catalysis: The Activation of Aryl Bromides. *Chemistry*, 21(44):15496–15501, 2015.

[75] A. Monguzzi, A. Oertel, D. Braga, A. Riedinger, D. K. Kim, P. N. Knüsel, A. Bianchi, M. Mauri, R. Simonutti, D. J. Norris, and F. Meinardi. Photocatalytic Water-Splitting Enhancement by Sub-Bandgap Photon Harvesting. *ACS Applied Materials & Interfaces*, 9(46):40180–40186, 2017.

[76] B. D. Ravetz, A. B. Pun, E. M. Churchill, D. N. Congreve, T. Rovis, and L. M. Campos. Photoredox catalysis using infrared light via triplet fusion upconversion. *Nature*, 565(7739):343–346, 2019.

[77] A. Tokunaga, L. M. Uriarte, K. Mutoh, E. Fron, J. Hofkens, M. Sliwa, and J. Abe. Photochromic Reaction by Red Light via Triplet Fusion Upconversion. *Journal of the American Chemical Society*, 141(44):17744–17753, 2019.

[78] B. Pfund, D. M. Steffen, M. R. Schreier, M.-S. Bertrams, C. Ye, K. Börjesson, O. S. Wenger, and C. Kerzig. UV Light Generation and Challenging Photoreactions Enabled by Upconversion in Water. *Journal of the American Chemical Society*, 142(23):10468–10476, 2020.

[79] L. Huang, L. Zeng, Y. Chen, N. Yu, L. Wang, K. Huang, Y. Zhao, and G. Han. Long wavelength single photon like driven photolysis via triplet triplet annihilation. *Nature Communications*, 12(1):122, 2021.